AIAA JOURNAL
Vol. 33, No. 3, March 1995

Perspective on Hypersonic Nonequilibrium Flow

H. K. Cheng
University of Southern California, Los Angeles, California 90089
and
G. Emanuel
University of Oklahoma, Norman, Oklahoma 73019

Introduction

ONGOING as well as new hypersonic flow programs continue to challenge the aerospace engineer. These programs are often of consuming difficulty, involving the synthesis of chemical kinetics, quantum mechanics, and radiation physics with fluid dynamics. To further complicate matters, the flowfield is often rarefied; thus the Knudsen number requires independent consideration along with the Mach and Reynolds numbers. Although these parameters are related, different regions of the flow, such as the interior of a bow shock, depend differently on them as compared with other regions.

Because of its complexity, recent research has focused on the modeling of more realistic, complex hypersonic flows with the intensive use of computational fluid dynamics (CFD). Of necessity, the large codes used in this effort must resort to various empiricisms and approximations. Our objective in this Survey is to discuss some of these empiricisms and approximations within the context of hypersonic nonequilibrium flow. The issues and advances examined are primarily chosen for their relevance to theoretical gasdynamics; however, this Review makes no claim to being comprehensive. The books by Anderson[1] and Park[2] provide background material for the discussion of current issues, including lessons learned from the design and operation of the Space Shuttle.

Our presentation is partly based on a previous report,[3] some of which was published elsewhere.[4] An alternative discussion of some of the same material can be found in an article by Tirsky[5] whose discussion is especially valuable for emphasizing hypersonic research by Russian workers, with greater emphasis given to engineering heat transfer predictions. Some of this work is not as well known in the western community as it should be. The importance of finite rate chemistry and the problem of fuel-air mixing to hypersonic airbreathing propulsion cannot be overemphasized.[6] These topics, however, are omitted from our discussion in as much as they fall under combustion gasdynamics and ought to be examined in this context.[7,8] The treatise on hydrogen combustion presented in Ref. 8 should be of interest to scramjet propulsion researchers. A broad perspective on hypersonic airbreathing vehicle design may be found in a survey (to be three volumes) edited by Bertin et al.[9]

In the next section, nonequilibrium aerothermodynamics is discussed. Much of this section is concerned with energy exchange that involves the vibrational modes of diatomic molecules. The subsequent section reviews the modeling of rarefied hypersonic flows and their continuum extension. There is no shortage of approaches that are available, as well as open issues. These approaches encompass the direct simulation Monte Carlo (DSMC) method, Navier–Stokes (NS) equations, Burnett, or augmented Burnett equations, and the 13-moment equations. The review concludes with a few brief remarks.

Nonequilibrium Aerothermodynamics

Current research developments in high-temperature flow physics still do not possess a methodology base with unquestioned certainty. A rational way to derive an equation set for a nonequilibrium flow is to write the time rate of population change of atoms and molecules, with a specific energy state i, as the difference between the sum of rates of all collisional and radiative transitions that populate a given state and the sum of rates that depopulate this state. Such a system is commonly referred to as the master equations; they furnish the source terms in the conservation equations for the species population of state i, N_i. The transition/emission rate for each collisional/radiative process is determined with the use of quantum me-

H. K. Cheng has been a professor in Aerospace Engineering at the University of Southern California for the last three decades and a Professor Emeritus since Fall 1993. He completed his BS degree in aeronautical engineering at the Chaio-Tung University, Shanghai, 1947, Ph.D. degree in aeronautics at the Cornell University, Ithaca, 1952, and subsequently worked at Bell Aircraft Corporation as a research aerodynamicist until 1956 when he joined Cornell Aeronautical Lab, Buffalo (predecessor of ARVIN-CALSPAN), and was a principal aerodynamicist of the laboratory after 1959. Dr. Cheng visited Stanford University as a lecturer in 1963–64. His research and teaching covers theories in subsonic, transonic, supersonic and hypersonic flows, rarefied gas dynamics, rotating and stratified fluid flows, as well as unsteady aero-/hydro-dynamics applied to animal flying and swimming. He is a Fellow in AIAA and APS, a member of the SIAM, Phi Tau Phi, and an elected member of the U.S. National Academy of Engineering.

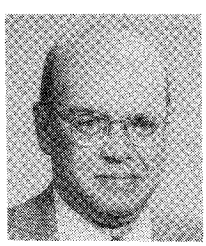

George Emanuel received a B.S. degree in mathematics from the University of California, Los Angeles, an M.S. degree in mechanical enginnering from the University of Southern California, and his Ph.D. in 1962 from Stanford University in aeronautical sciences. Subsequently, he spent nine years at The Aerospace Corporation, four years with TRW, and four years at the Los Alamos National Laboratory. He was a member of the technical staff at Aerospace and TRW, where his research and administrative duties primarily involved CW and pulsed, high energy chemical lasers. He published the first computer simulation of this laser. At LANL, he was staff to the applied photochemistry division with responsiblity for the physics, system, and econamics modeling of a new uranium enrichment process. Since 1980, he has been a professor of aerspace and mechanical engineering at the University of Oklahoma. He is the author of *Gasdynamics: Theory and Applications* and *Advanced Classical Thermodynamics*, both published by the AIAA education series, and, in 1994, *Analytical Fluid Dynamics*, published by the CRC Press. This is his 22nd article to appear in this journal; he is an Associate Fellow of AIAA.

Received March 15, 1994; revision received July 11, 1994; accepted for publication July 13, 1994.

chanics for the molecular, atomic, and electronic interactions and with the detailed balance hypothesis.[2,10] This hypothesis, it should be noted, still requires rather bold assumptions regarding the interaction potentials and the collision mechanism, as discussed later.

Vibrational Relaxation/Excitation and Dissociation

At relatively low temperatures, vibrational excitation is considered the main channel of energy transmission to the upper levels. This process thus controls the rate of dissociation. For the study of vibrational nonequilibrium, radiative transitions are considered to be much slower than those by collisions and are often deleted from the master equations governing the vibrational transitions.[2]

In the theory for vibration-translation (V-T) energy exchange, the rates of state-to-state transitions are furnished by modeling collisional and excitation processes. These may lead to quite different results depending on the form of the intermolecular and interatomic potentials and other approximations that are used. Consider an end-on collinear (aligned, one-dimensional) collision of a rotationless *harmonic-oscillator* molecule, which has equal spacing between neighboring levels, with an atom or a molecule that has a frozen vibrational energy, and assume an exponentially decaying interaction potential as in the Landau–Teller[11] theory. One finds that transitions can occur only to neighboring states ($v \rightarrow v \pm 1$) with a deactivating transition rate proportional to the vibrational quantum number v. This leads to the familiar relaxation equation for the average vibrational energy, namely,

$$\frac{\partial}{\partial t}\bar{\epsilon}_v = \tau^{-1}[\bar{\epsilon}_v^*(T) - \bar{\epsilon}_v]$$

where $\bar{\epsilon}_v^*$ denotes the average equilibrium vibrational energy at the translational temperature T of the heat bath. The temperature and pressure dependence of the vibrational relaxation time τ for a number of air-species pairs are estimated and correlated with experimental data at temperatures up to 5000 K by Millikan and White[12] and others.[2] Presumably, the V-T mechanism is appropriate when most of the molecules are in the ground vibrational state and thus involve little vibration-vibration (V-V) energy exchange.

When excited vibrational levels are populated, V-V energy exchange must be considered and is generally believed to be much faster than that by V-T. In their analysis, Schwartz, et al.[13] (SSH) consider an end-on collinear collision model of a pair of diatomic molecules, for which the vibrational energies in both can be altered, again assuming no rotational energy exchange. A separable form for the *intermolecular* potential

$$U \propto \exp[-\alpha(r - \beta_A r_A - \beta_B r_B)]$$

is used, where r_A and r_B are the internuclear separations for molecules A and B, respectively, and r is the distance between the mass centers of the two molecules. According to the SSH analysis for a harmonic oscillator, the contribution to the rate of transition caused by vibrational energy exchange during a collision differs substantially depending on whether the total internal energy change $\Delta E = (E_A' + E_B') - (E_A + E_B)$ is (nearly) zero or not. The contributions from resonant V-V collisions, corresponding to $\Delta E \cong 0$, are predominant and thus preferential.[2] An equal energy level spacing makes this type of exchange possible, although it is not strictly applicable to a more realistic anharmonic oscillator. Nevertheless, the V-V mechanism is expected to dominate among the lower vibrational levels where a nearly uniform spacing prevails.

With regard to anharmonicity, the study by Treanor et al.[14] should be recalled (also see the review by Rich and Treanor[15]). With V-V exchange limited to $v \rightarrow v \pm 1$, and assuming the V-T transitions are generally much slower than V-V transitions, these authors obtain a quasi-steady-state (QSS) solution to a V-V dominated master equation

$$N_v \approx N_0 e^{-\gamma v} \exp(-E_v/kT) \qquad (1)$$

where N_0, γ, and T may vary slowly with time at a rate comparable to the V-T rate. This result can be recast into a form alluded to as a "Treanor" distribution

$$N_v \approx N_0 \exp(-vE_1/kT_v)\exp[(vE_1 - E_v)/kT] \qquad (2)$$

For a harmonic oscillator, the distribution in Eq. (2) is Boltzmann at a vibrational temperature T_v, but for an anharmonic oscillator, the last factor furnishes a needed correction. For $T < T_v$, corresponding to a sudden decrease of the translational temperature from an equilibrium value, γ is negative and Eq. (1) signifies an excess population, adding to the potential for a population inversion. In a low-temperature range, their study[14] indicates a relaxation time much shorter than that for a harmonic oscillator. Calculations should be performed with an extended anharmonic version of the SSH theory that includes molecular rotation for the species: O_2, NO, CO, OH, H_2, and N_2. For an expanding flow, however, this has been carried out by Park,[16] Ruffin and Park,[17] and de Roany et al.,[18] confirming the essence of the previous non-Boltzmann distribution. The V-V dominance underlying Eqs. (1) and (2) may not hold at higher vibrational levels, where a more drastic departure from a Maxwell–Boltzmann distribution occurs, as discussed shortly.

The SSH analysis, when extended to models with anharmonic oscillators and dissociation, yields quite different results, as may be seen from the Sharma et al.[19] study and as elucidated by Park.[2] The nonuniform vibrational energy spacings are calculated for several intermolecular potential models, including the Sorbie–Sorret and two-term Dunham potentials; multiquantum $v \rightarrow v \pm 2$ transitions are also considered. The overall transition rate coefficients, $K(v, v+1)$ and $K(v, v+2)$, as well as $K(v, c)$, were computed up to the vibrational level $v = 50$ for rotationless N_2 at $T = 8000$ K and $T_v = 4000$ K. Here, $K(v, c)$ is the rate coefficient for the transition from vibrational state v to a dissociated state, which is unaccounted for in Treanor et al.[14] The case considered, with $T > T_v$, corresponds to a sudden heating of the gas, such as that occurring behind a shock. Interestingly, the calculation indicates a vibrational excitation "bottleneck" around $v = 20$, where $K(v, v+1)$, as well as a second moment of $K(v, v')$ has an extremely low minimum (reproduced in Figs. 2.10 and 3.3 of Ref. 2). With this set of $K(v, v')$ and $K(v, c)$, the time-dependent master equation yields an evolutional solution for N_v that is non-Boltzmann with three distinct v ranges. In this case, the bottleneck inhibits the transfer of vibrational energy to the upper states. For this non-Boltzmann result, Sharma et al.[19] computed the rate of total vibrational population removal, i.e., the forward dissociation rate k_f, as well as the rate of total vibrational energy loss, or the average removed vibrational energy.

With a non-Maxwellian vibrational distribution, the dissociation rate coefficient k_f of the diatomic species and the associated *rate of vibrational energy removal* $\bar{\epsilon}_v$ must be weighted by the appropriate nonequilibrium distribution. Average values may result that differ considerably from conventional estimates (cf. pp. 104–115 of Ref. 2), thereby reflecting a vibrational temperature T_v that is different from the translational temperature T. Hammerling et al.[20] calculated $k_f(T, T_v)$ with vibrational nonequilibrium for the radiation behind a shock in nitrogen. They stipulate that the low-lying energy states can be described by a local Maxwellian with $T_v \neq T$, whereas a QSS approximation is used for the high-lying states. This type of model is considered to be non-quasi-steady, the result for $k_f(T, T_v)$ is called the coupled-vibration-dissociation (CVD) model.

Under the QSS approximation with a rotationless harmonic oscillator model, which leads to a Maxwellian distribution, Treanor and Marrone[21] evaluated the rate of average energy loss to be one-half of the dissociation energy, measured from the ground state, i.e., $\bar{\epsilon}_v = D/2$. A subsequent non-Maxwellian distribution study[22] suggested that $\bar{\epsilon}_v$ should be $D/2 \leq \bar{\epsilon}_v \leq D$. This is because bound-free transitions more readily occur from the more densely populated high-lying states of an anharmonic oscillator. This preference for bound-free transitions from the higher states is referred to as *preferential dissociation*.

Sharma et al.,[19] however, concluded that $\bar{\epsilon}_v$ is less than $D/2$ for an anharmonic oscillator, i.e., $\bar{\epsilon}_v \cong 0.3D$. (We further comment on this shortly.) Despite these disparate $\bar{\epsilon}_v$ estimates, the removal upon

dissociation of vibrational energy is large compared with the average vibrational energy itself, which generally is much less than D.

As pointed out by Gonzales and Varghese,[23] these extended SSH results are affected by uncertainties related to a number of assumptions made by Sharma et al.,[19] where corrections for several errors and three-dimensional effects in the original SSH analysis[24,25] are not included. Another issue is the distorted wave approximation implicit in the SSH theory, which may not be appropriate for transitions involving large relative velocities and multiquantum transitions.[10] A more recent study by Landrum and Candler[26] on vibration-dissociation coupling in N_2 used a corrected and updated version of the SSH theory, including contributions from collinear collisions of diatomics and atoms. The important range parameter α of the intermolecular potential, however, appears to be improperly determined with the Murrell and Sorbie potential, which, according to Gonzales and Varghese,[23] is appropriate only for the field between bound atoms. Thus, a demonstration of the existence of the bottleneck has not been established. It should be pointed out that a DSMC calculation by Olynick et al.,[27] using inelastic cross-section data corresponding to the rates used in Sharma et al.,[19] gives no sign of a bottleneck.

The master equations for the vibrational state population distribution that also allows transitions to the unbound (dissociated) state may be approximated by an integral equation. With appropriate assumptions, the latter may in turn be reduced to a diffusion-like equation,[28] which is discussed here for its theoretical importance in the interpretation of computational and experimental results. If the vibrational energy gap $E(v+1) - E(v)$ is small compared with kT, the master equation for diatomic molecules may be expressed in an integral equation form (we mostly use Park's[4] notation)

$$N_x^{-1}\frac{\partial}{\partial t}\rho(v) = \int_0^{v_m} K(v, v')[\rho(v') - \rho(v)]\,dv' + K(v, c)\,[\rho_A\rho_B - \rho(v)] \tag{3}$$

where v and v' are the vibrational level numbers; N_x is the number density of the colliding partner; ρ is the number density of the v level normalized by its equilibrium value, i.e., $\rho \equiv N_v/N_v^*$; ρ_A and ρ_B are the normalized number densities of the (free) atoms A and B; and v_m is the maximum v value. Two additional requirements are needed in the diffusion theory. They amount to 1) the rate $K(v, v')$ is large only in the vicinity of $v' = v$, and 2) $K(v, c)$ is appreciable only for upper states near the dissociation limit. Note that a typical midlevel vibrational energy is on the order of the dissociation energy D and that in most cases of interest $kT \ll D$. This, together with the assumption required for the integral form of the master equation, means

$$\Delta E \equiv E(v+1) - E(v) \ll kT \ll D \tag{4}$$

Since the kernel $K(v, v')$ is sharply peaked under assumption 1, Eq. (3) simplifies to

$$N_x^{-1}\frac{\partial}{\partial t}\rho(v) = \frac{\partial}{\partial v}\left[M\frac{\partial}{\partial v}\rho(v)\right] + K(v, c)[\rho_A\rho_B - \rho(v)]$$

where M is a transition moment

$$M(v) \equiv \int_{-\infty}^{\infty} K(v, v+\xi)\xi^2\,d\xi$$

If high-lying v states with energy $E(v)$ close to the dissociation limit are excluded, then a diffusion equation follows,

$$N_x^{-1}\frac{\partial}{\partial t}\rho(v) = \frac{\partial}{\partial v}\left[M\frac{\partial}{\partial v}\rho(v)\right] \tag{5}$$

by virtue of Eq. (4) and assumption (2). The boundary condition at $v = 0$ is $\partial\rho/\partial v = 0$, since no molecules can cross this boundary. The upper boundary condition at $v = v_m$ is furnished by Keck and Carrier[28] as

$$M\frac{\partial\rho}{\partial v} = (\rho_A\rho_B - \rho)\int_0^{v_m} K(v, c)\,dv$$

An ambiguity appears, since the right side of this relation is seen to be the net formation rate of molecules from atoms. A more in-depth discussion on the boundary conditions is given in Park.[16] Equation (5) shows that a vanishingly small diffusion coefficient M at a middle level would inhibit the upward population migration to the dissociation level and would signify the bottleneck noted earlier. The $M(v)$ in the example of sudden heating of N_2 in the study by Sharma et al.[19] did reveal an extremely low minimum, as mentioned. This latter result would have had a theoretical impact if not for the uncertainties brought out earlier.

An interesting application of diffusion theory has been made by Lee,[29] who considers a model of energy exchange of vibrational oscillators with an electron heat bath in the absence of dissociation. This model has been considered important in the study of a highly ionized re-entry flow.[30] Reasonable agreement is demonstrated between the diffusion model and the original discrete master equations in the sudden-heating case. Non-Boltzmann distributions are shown at an early stage of the transient, but a bottleneck in $K(v, v')$ is not evident.

Transition rate calculations can be improved by using an extension of the semiclassical N state method[31] in which the dynamics of the colliding pair are modeled classically, whereas the oscillator motion is modeled quantum mechanically. The task is computationally intensive; only a few of the many needed state-to-state V-V transition rates have been calculated by Gonzales and Varghese.[23,32]

Another semiclassical approach is being developed by Kunc,[33] who treats V-T exchange for diatomic species based on a multicenter potential model developed earlier.[34] The treatment includes a quantum mechanical interaction of vibration and rotation. Sample rotational transition probabilities $P_{j,j-1}$ have been computed for $j = 1, 4$, and 20 of N_2 and O_2. Comparison with the collision numbers for the $v = 1 \rightarrow 0$ transition, Z_{10}, inferred from existing experimental data (after adjusting a constant g in the theory), shows encouraging agreement in the temperature range of 1000–6000 K. Comparisons of this approach with experiment and with other theories for transition rates at the higher vibrational levels remain to be made. It is also unclear if V-V exchange, not considered in Ref. 33, may also be described adequately by a multicenter model.

The relative importance of the V-T and V-V mechanisms is elucidated by Rich and Macheret.[35] They discuss recent experimental and theoretical developments in electric discharges, in expanding flows, gasdynamic flows with shock waves, and in optically pumped cells. The vibrational energy levels of the anharmonic vibrator are modeled as

$$E_v = T_e + \omega\left(v + \tfrac{1}{2}\right) - \chi\omega\left(v + \tfrac{1}{2}\right)^2 \tag{6}$$

where T_e is the electronic energy, ω is the fundamental vibrational frequency, and χ provides an anharmonicity correction. With Eq. (6), the QSS solution of the master equations is obtained after omitting contributions from exchanges with other electronic states, spontaneous radiative processes, chemical reactions, resonance laser radiation, and other sources of vibrational pumping. The solution recovers the Treanor distribution, Eq. (2), which is maintained by the dominant V-V process. The distribution, however, has a minimum at a $v = v_0$ value, beyond which the V-T contribution becomes equally important. For $v > v_0$, Gordiets and Mamedov[36] provide an expression that complements Eq. (2). From gases such as N_2 and CO, it predicts a gently falling "plateau" region, e.g., $N_v \sim (v+1)^{-1}$.

A similar analysis of the V-V, V-T kinetic rate models was independently presented by Lam.[37] Under strongly pumped QSS conditions, three v ranges are identified: 1) Treanor ($0 \le v < v^*$), 2) plateau ($v^* \le v < v^{**}$), and 3) quasi-Boltzmann ($v^{**} \le v$). The transition values v^* and v^{**} can be analytically described. Comparison of this asymptotic theory with a numerical solution to the master equation for a 1: 9 CO-He mixture at 100 K is encouraging. The measured nonequilibrium vibrational state populations for N_2, NO, and CO, using different excitation techniques, are shown in Fig. 1. These results are strikingly similar to the foregoing description.

The analyses of Refs. 14, 36, and 37 are limited to an anharmonic model, such as Eq. (6), and are not appropriate for the levels near the dissociation limit. For nonequilibrium dissociation, Macheret

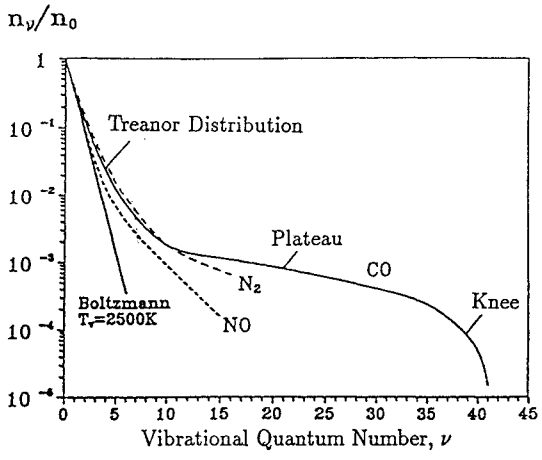

Fig. 1 Measured nonequilibrium vibrational state populations in diatomic gases (from Rich and Macheret[35]). The N_2 data are from pulsed electric discharge excitation, the NO data from direct current electric discharge excitation, and the CO data from excitation by a CO infrared laser.

and Rich[38] provide a physical model that is claimed to be nonempirical. The theory yields an analytical formula for the rate coefficient $k_f(T, T_v)$ for the $X_2 + M \rightarrow 2X + M$ dissociation process. For N_2-N_2 collisions, it differs significantly from the corresponding coefficients from Park[16] and from the Treanor–Marrone[21,22] CVD model in the 1000–7000 K T_v range at $T = 10{,}000$ K.

Electronic Excitation and Ionization

Several available computer codes for predicting radiation intensities from flows in thermochemical nonequilibrium, such as the nonequilibrium radiation program (NEQRAP) and the nonequilibrium air radiation (NEQAIR) codes, are based on the QSS model of the master equation for atomic electronic states, which determines the N_i in terms of a free-electron temperature T_e and the electron number density N_e. The latter is determined separately by a rate equation. In NEQAIR, it is assumed that the system can be characterized by three temperatures: T_e, T_v, and T. The vibrational temperature T_v is shared by all molecules, and the translational temperature T is shared by all heavy particles. These models utilize an atom or molecule ionization potential that represents the energy difference between the ionized state and the electronically excited states.[39] Moreover, behind a strong shock or during recombination in a rapid expansion,[40] the electronic states have a non-Boltzmann distribution. The kinetic rates may be coupled to those for the other processes. For instance, Gally and Carlson[41] obtain reverse rates from equilibrium constants based on species partition functions. In turn, the partition functions are calculated using the T, T_v, and T_e temperatures.

Much of the radiative heat transfer modeling has been to replicate the flight integrated re-entry environment (FIRE II) experiment. In a recent study, Greendyke and Hartung[39] found that all versions of the radiative heat transfer calculation method, both coupled or uncoupled, overestimate the radiative intensity at the most nonequilibrium condition by more than 100%. The same codes tend to underestimate the radiative intensity at equilibrium conditions. The more accurate methods couple the radiation model to the chemical and fluid mechanic models. Although coupled and uncoupled profiles are similar, coupling reduces the temperatures in the shock layer through radiative cooling and results in a reduced radiative heat transfer. In some cases, this reduced heat transfer is approximately 20% below the experimental values. Radiative heat transfer is further discussed in a subsequent section.

Applications and Assessment

Studies of the vibrational transition model have led to an appreciation of the multiple-temperature concept in nonequilibrium aerothermodynamics. These improvements in concept take the form of allowing several independent temperatures, namely, the translational-rotational temperature T shared among heavy particles, the vibrational temperature T_v shared by all molecules, and (depending on the requirement) the electron-electronic temperature T_e. These temperatures appear in the empirical rate formulas and reflect on the impact of T, T_v, and/or T_e as suggested by the model studies. The rate of vibrational energy change due to collisions may be evaluated as a sum contributed to by three sources: 1) the Landau–Teller[6] form for V-T and V-V transitions modified by a factor depending on T_v and T, 2) vibrational excitation contributed by electronic impact (significant for N_2), and 3) vibrational energy removal/addition due to dissociation/recombination, with an average energy per molecule $\bar{\epsilon}_v$ based on some dissociation model. This sum enters as a source term in the partial differential conservation equation governing E_v. Similarly, the rate of the electronic energy change E_e is contributed to by seven kinetic processes that result from electronic excitation, ionization, ionic recombination, radiation, etc. This rate enters as a source term in the conservation equation for E_e.

Empiricism is found in the attempt to modify the pre-exponential temperature dependence in the forward reaction rate k_f by replacing T with the product of an average[4]

$$T_a = T_v^q T^{1-q} \tag{7}$$

where q varies between 0 and 0.5 in practice. The lack of adequate experimental data to determine the constants and exponents of the rates represents a considerable uncertainty. In this regard, Tirsky et al.[42] have computed the heat flux along the Buran spacecraft re-entry trajectory using six different sets of kinetic rates, including those discussed here. Although these rates significantly differ from each other, the heat flux variation is only 30%. Thus, the engineering value of complicated kinetic models with adjustable parameters is also uncertain. The tendency for ever more complicated models, of course, is fueled by our steadily increasing computational capability.

Another area of ambiguity concerns transport properties of the gas mixture and its simplification,[43,44] which has not been critically tested or evaluated in the elevated temperature range of interest. The need for scrutiny is apparent by the example of iodine vapor considered by Kang and Kunc[45] and Kunc.[46] According to their model, the viscosity μ of dissociating iodine in the range from 10^3 to 2×10^3 K should yield a negative slope, i.e., $d\mu/dT$ is negative. This would be significant for flow stability studies. Similar properties could occur for other dissociating or ionizing species. We note that the semi-analytic formula for μ in Ref. 46 is rather explicit and hence useful, but that experimental evidence is needed to substantiate this intriguing theoretical finding. It would be of interest to see if this slope reversal also occurs in the heat conduction and diffusion coefficients.

Gupta[47] studied the thermochemical and radiative properties of the shock layer for the FIRE II experiment carried out during a Space Shuttle flight.[48] Solutions are obtained with the NS equations and nonequilibrium chemistry and also for the viscous shock-layer (VSL) equations but with equilibrium chemistry. Except at altitudes higher than 80 km, the FIRE II data of radiative intensity and heat flux agree reasonably well with equilibrium VSL solutions for a fully catalytic surface as well as the inviscid shock-layer and boundary-layer analyses of Sutton.[49] In a code-calibration study, Gnoffo[50] applied the Langley aerothermodynamic upwind relaxational algorithm (LAURA) code using Park's 11-species model[2] with $q = \frac{1}{2}$ to predict the convective heat transfer rate of the FIRE II test during the early test period (corresponding to 11.3 km/s at an altitude of 85–67 km). Good agreement with flight test data is found, although the heating rates in this range are too small, compared with those at lower altitudes, to be of significance.

In a proposed aeroassist flight experiment (AFE), Hamilton et al.[51] predicted the stagnation point heating history of a fully catalytic heat shield with a 2.2-m nose radius using an 11-species nonequilibrium air chemistry model and the VSL approximation. Peak convective heating in this case occurs at 78-km altitude at a speed of 9.2 km/s. The predicted value reaches 0.5 MW/m^2, which is believed to be the limit for the reusable tiles on the Space Shuttle. However, this VSL analysis ignores the shock-slip correction, which would result in a 50% reduction of the peak value, as discussed in the next section.

Radiative heating dominates the surface heat flux at appreciably higher re-entry velocities and at lower altitudes and on a larger

body, such as during an aerobraking return from a Mars mission. In this case, a coupled radiation and ablation injection model of the nonequilibrium viscous shock layer is used in a re-entry heating study by Gupta et al.[52] assuming a speed of 16–8 km/s, an altitude of 80–65 km, and a nose radius of 3 m. The study extended an earlier work of Moss[53] and assessed the impact of using different transport and thermodynamic properties, and also different radiation models and, interestingly, showed the adequacy of a universal Lewis number of 1.40. Over the speed range of 16–12 km/s, the wall-heating rate is found to vary from 2.5 to 11 MW/m^2 with radiation contributing 40–70%; the effectiveness of ablative injection of a carbon-phenolic compound is unclear from the study. Entry into a Martian atmosphere represents a different aerothermal environment, where CO_2 (97%) and N_2 (3%) are the main constituents. Estimates for entry vehicles with nose radii varying from 1 to 23 m indicate the need for considering a speed range of 6–12 km/s at altitudes of 30–50 km. Candler[54] and Park et al.[55] have studied the nonequilibrium nature of this problem. Candler's NS calculations, based on an eight-species chemistry model without ionization, reveal near thermochemical equilibrium in most parts of the shock layer, attributed to fast CO_2 vibrational relaxation. Applying a computationally more efficient VSL analysis to this problem, Gupta et al.[56] assume full thermochemical equilibrium but allow coupling of the shock-layer thermodynamics to radiative cooling. Their results in the lower speed range (6–6.5 km/s) support Candler's observation on chemical equilibrium. Convective heat transfer at an 8-km/s speed contributes 60% of the total heat flux for the 1-m nose radius and 23% for the 23-m nose radius; at 12 km/s it amounts to only 40% for the 1-m nose and 2.4% for the 23-m nose radius.

A series of instrumented probes, called the radio attenuation measurement C (RAMC) experiment, have flown at 7.65 km/s and at altitudes of 71–81 km to measure the electron number density around a sphere cone with a 0.152-m nose radius.[57] Gnoffo[50] compared his LAURA calculations of the electron number density profile using two sets of chemical kinetic rates with data measured by a Langmuir probe rake. Only qualitative agreement is achieved, e.g., see, Fig. 13 in Ref. 50. An earlier VSL calculation by Kang et al.[58] showed better agreement with the measured data. The discrepancy is believed to have resulted from the assumption in LAURA of a fully catalytic surface, which perhaps is inappropriate for a Teflon-coated afterbody.

The electron number density in a shock layer caused by thermal ionization can be determined with the quasineutral approximation and a related ambipolar-diffusion model.[2,59,60] In passing, we note that Ref. 60 provides a helpful introduction to the fundamentals of high-temperature flowfield analysis, including radiation, of hypervelocity atmospheric flight. Recently, Qu et al.[61] examined the effect of several versions of this model for flow along the stagnation streamline with a freestream speed of 7.6 km/s in a standard atmosphere for Reynolds numbers of 8×10^2 and 4×10^3. The air model consisted of seven species (N_2, O_2, N, O, NO, NO^+, and e^-). In the NO^+ and e^- conservation equations, the net fluxes of electric charges are set equal to zero. Although these approximations break down within a Debye shielding distance from the wall, the calculation reveals a large reduction in the electron density of more than 1000 relative to a purely quasineutral calculation.

Candler and MacCormack[62] assumed a noncatalytic wall in a NS calculation for the RAMC tests and found reasonable agreement for the electron number density with the microwave-reflectometer data measured along the cone's afterbody (cf. Figs. 2–4 therein). Two sets of chemical kinetic models were tested: one consisted of five species, N_2, O_2, NO, N, and O; the other consisted of two more species, NO^+ and e^-. The electron density in the five-species set is generated by a special quasisteady approximation that proves to be inadequate. The treatment of nonequilibrium flow models are similar to those of Lee[30] and Park.[2] The program allows distinct vibrational temperatures for different molecular species, which turned out to be close to one another, thus supporting Park's idea of a common T_v shared by all molecules.

With a two-temperature version of the LAURA code, Greendyke et al.[63] carried out a parametric study of the unknown procedure constants/exponents in the nonequilibrium thermochemical models and their impact on the electron number density prediction for the AFE experiment. Variations are considered in the reference ionization potential of N and a selection of rate constants from among Dunn and Kang,[64] Park,[2,65] and their updates, including the options of using the Ref. 52 equilibrium constants and also imposing limiting cross sections for vibrational excitation. A value for the exponent q in Eq. (7) proposed by Hansen,[66] $q = 0.1 + 0.4(T_v/T)$, is also considered; in this case it appears to yield only minor changes. The calculations made for an AFE model (2.16-m nose radius at an altitude of 78–81 km with a speed of 9.7–8.9 km/s) reveal a significant variation in the rate of electron impact ionization with a correspondingly large difference in the location and magnitude of the peak electron density. The severity of an electron avalanche associated with changes in these models is noted.

Hartung et al.[67] performed an extensive parametric study using the two-temperature version of the LAURA code. They studied radiative emission profiles and radiation spectra in the stagnation region for conditions corresponding to a FIRE II flight experiment (altitude of 76–85 km, speed of 11.4 km/s, nose radius of 0.75 m). The radiation model is the Langley optimized radiative nonequilibrium (LORAN) code, which yields results that differ little from Park's NEQAIR results.[2] A sensitivity study again includes the choice of the exponent q for the dissociation rate and of a limiting vibrational relaxation cross section, both of which are shown to be critical. Mitcheltree[68] examined LAURA solutions for the translational and vibrational temperatures, electron number density, O_2 concentration, as well as convective and radiative surface heating rates. The flow condition in the study corresponds to an aerobrake with a 1-m nose radius at 12 km/s and an 80-km altitude. Rate parameters variations are seen to have an effect, as large as a factor of 3, on the degree of ionization and radiative heating. The results based on Park's[2,65] rate sets are seen to be little affected by using the Gupta et al.[52] equilibrium constants; Hansen's model[66] for q appears to give results virtually identical to that for $q = 0$.

Hartung[69] pointed out that the procedure in Park's NEQAIR code may lead to a negative excitation temperature for a bound-free transition, which is avoided in LORAN. Her comparison of the predicted emission spectrum in the visible range from LORAN with an AVCO shock tube experiment[70] at the condition corresponding to the peak radiation point does not appear to be as good as expected, thus requiring further study. On the other hand, there is better agreement of the NEQAIR prediction with the AVCO emission measurement found earlier by Park[65] both in the equilibrium and nonequilibrium regions (see also Fig. 8.24 in Ref. 2). The comparison is reproduced in Fig. 2, where the dashed curves are results from DSMC models, which are discussed in the next section.

Modeling of Rarefied Flows and Their Continuum Extension

Because of space limitations, the following discussion focuses on the continuum extension for hypersonic flows and aspects of the DSMC as a predictive tool. Broader perspectives on rarefied gasdynamics (RGD) are offered in earlier volumes of the *Annual Review of Fluid Mechanics*.[71–74] More recent works and reviews can be found in the 1989 and 1992 RGD proceedings. A review of numerical simulation of rarefied hypersonic flows by DSMC calculations and a comparison with Shuttle re-entry data were presented by Lin et al.[75]

DSMC as a Predictive Tool

The basic ideas of the DSMC method and numerical procedures are described in the Bird monograph,[76] and are further elucidated in several reviews.[73,77–79] Although the statistical errors present in a solution are expected to be inversely proportional to the square root of the total number of simulated particles, $N^{-\frac{1}{2}}$, an essential feature of the DSMC procedure is that the computational work is proportional to only the first power of N. The computer resource for a two-dimensional analysis is generally manageable in many institutes and universities but is still much larger than that required

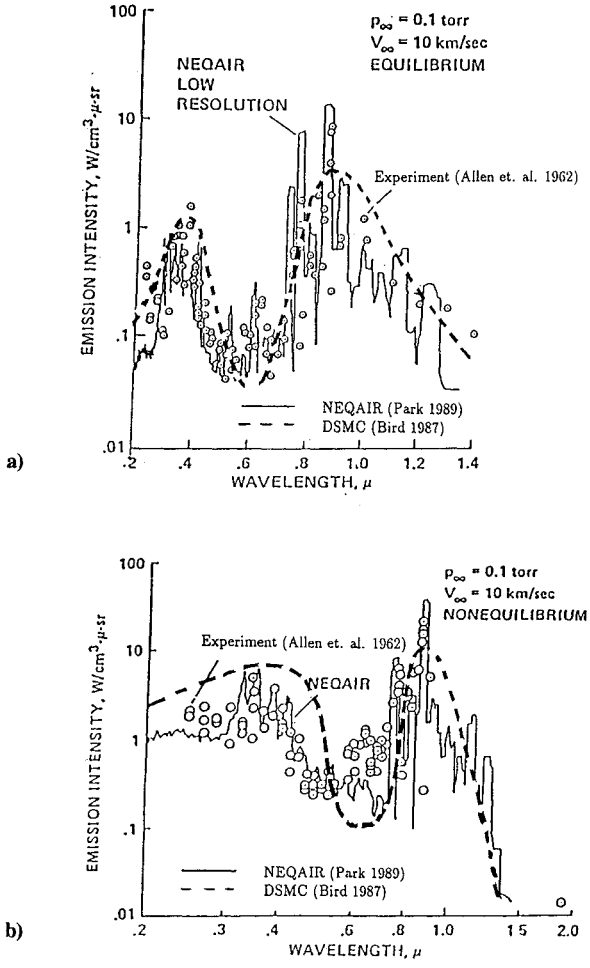

Fig. 2 Comparison of calculated and measured spectra for air behind a normal shock (from Park[49]), where the shock speed is 10 km/s and the upstream pressure is 0.10 Torr: a) the near equilibrium region well downstream of the shock and b) the nonequilibrium region just downstream of the shock. Emission spectra based on Bird's[92] DSMC-VHS model are shown as dashes.

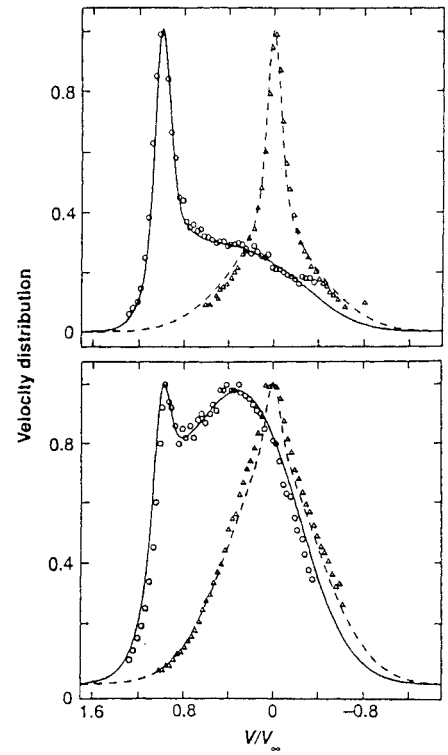

Fig. 3 Predicted and experimental velocity distributions (from Phan-Van-Diep et al.[111]): a) $\tilde{n}$ = 0.285 and b) $\tilde{n}$ = 0.565. Experimental data are represented by the symbols, whereas DSMC $f_\parallel$ and $f_\perp$ are the solid and dashed curves, respectively.

for a NS calculation. Variants of this method have been developed for improved computational performance with vector and parallel-processing computer architectures.[80–84]

A novel feature that greatly increases the computing speed of a DSMC program is the variable-hard-sphere (VHS) model, which treats the interaction of the molecules as a collision between two rigid spheres. This allows the postcollision relative velocity to be sampled from a uniform distribution in solid angle, whereas the sphere radius is allowed to vary with the relative speed c_r, which may preserve the correct viscosity-temperature relation under translational equilibrium. Hence, the cross section is proportional to $c_r^{-2\omega'}$, where $\omega' = \omega - 0.5$, and the viscosity is proportional to T^ω.

An extension to molecules with rotational and vibrational excitation is made with the Borgnakke–Larsen[85] (BL) phenomenological model, in which a fraction of a collision is assumed elastic and the remainder inelastic. New values of the internal and translational energies are then sampled from an equilibrium distribution to be taken as the postcollision particle properties pertaining to the inelastic fraction. The characteristic collision number Z for internal energy relaxation is roughly taken as the reciprocal of the inelastic-collision fraction and may be chosen to match a relaxation time estimate from experiment. The collision number Z is commonly taken to be 5 for rotation and 50 for vibration. In the DSMC calculation for a shock front, Olynick et al.[86] took into account the temperature and pressure dependence of the relaxation collision number in accordance with rates used in the continuum model. Additionally, Boyd[87] derived a velocity-dependent collision number, which gives results in accordance with those of Parker.[88] In Ref. 82, Boyd bypasses the BL model with a vibrational relaxation model for VHS application by modifying the Landau–Teller[6] theory. This approach succeeds in determining vibrational cross sections for (one-step) activation and deactivation that turns out to be independent of the intermolecular collision model. The model compares well with one available experiment and represents a more detailed predicting method than the BL model. An alternative modification of the BL model was offered by Chung et al.[89] for a gas mixture that assumes a combination rule for the effective collision cross sections.

A form of the collision theory of chemical physics that is consistent with the VHS model is used to convert the temperature-dependent rate constants to collision energy dependent reaction cross sections.[62–64] Ambiguity in modeling a three-body collision arises. The latter, however, may not be of great concern for DSMC applications, since the binary-scaling law prevails in many cases for nonequilibrium flows of interest.[90–92] A BL-type equilibrium distribution for the reaction products is assumed; whether the model may allow a vibrational-temperature dependence for the reaction rate is unclear.

A similar idea can be adopted in an extension of the DSMC to nonequilibrium flows with radiation. Apart from issues concerning the BL model, the task of tracking the large number of electronic states and of adjusting the constants for each rate to match data from available experiments and other continuum-based rate sets would appear to be insurmountable. Nevertheless, this task was accomplished and is documented in detail.[92,93] As validation, Bird[92] compares the spectral distribution of emitted radiation determined by an 11-species air chemistry calculation for the AVCO experiment shown as Fig. 2. The thick dashes represent his results and appear to successfully capture the trends, even in the nonequilibrium flow region. Inasmuch as the number of adjustable constants in the program is huge, an extensive sensitivity study should be in order. Such an investigation is performed in part in Carlson and Hassan's[94] study, where a scheme is introduced to determine the relaxation collision number Z_e for electronic-state excitation, which may reduce the degree of empiricism in the DSMC radiation model.

Bird's DSMC radiation model is applied by Moss et al.[93] to predict

the history of radiative and convective heating for an AFE vehicle, which was investigated earlier by Hamilton et al.[51] using various versions of continuum models. Flight conditions correspond to an altitude of 78–90 km and a speed of 7.6–9.9 km/s, for which radiative heating is found to be negligible compared with convective heating. It becomes noticeable but still small during the peak heating period, where the stagnation convective and radiative heat fluxes are 0.19–0.21 MW/m^2 and 0.03–0.04 WM/m^2, respectively. These values are lower than a corresponding continuum VSL prediction by a factor of 0.40. The discrepancy is believed to have resulted from the omission of "shock slip" in the VSL method, as discussed later.

A number of comparisons of DSMC calculations with experiment can be found in the 1990 RGD proceedings. Aside from these, there are several notable examples of comparisons from more recent studies, to be described in the following four paragraphs.

The steady expansion of nitrogen from a 20-deg nozzle to a near vacuum (with a throat Knudsen number of 2.3×10^{-3}) is investigated experimentally and computationally[95] using NS and DSMC. Consistently good agreement is found between the DSMC calculations and the pitot pressure and flow angle measurements inside and downstream of the nozzle. Although the solution is sensitive to the surface-interaction model, the fully diffuse wall model appears to be quite satisfactory. Pham-Van-Diep,[96] Boyd et al.,[97] and Pham-Van-Diep et al.[98] infer both rotational and vibrational state populations of pure iodine vapor at a location along the symmetry axis of an exhaust plume of I_2 flow in a wind tunnel. The population distributions inferred are close to those of a Maxwell–Boltzmann distribution among the 20–120th rotational levels and among the 0–4th vibrational levels at $T_v \cong T_r > T$. The data appear to support Treanor's V-V dominated model under a small anharmonicity, although the extent to which the observed feature was influenced by the freezing phenomena common to an expanding supersonic nozzle flow is not clear.

Severe interference heating at a scramjet cowl lip, associated with the Edney Type IV shock configuration,[99] is analyzed by Carlson and Wilmoth[100] with DSMC calculations using 4×10^5 simulated molecules. The peak heating rate obtained appears to be considerably lower than the experimental value, $q/q_0 \cong 30$.[101] As the authors note, the grid/cell system employed may not be adequate, and a full NS calculation should be made for this case. Not considered is the possibility of an unsteady flow, in which the time-averaged heat transfer rate may substantially exceed that of a steady flow. This possibility can be analyzed with a time-accurate unsteady calculation.

Discrete simulation Monte Carlo calculations have been made by Dogra et al.[102] that are compared with hypersonic sphere drags at low Knudsen numbers ($M_\infty = 11$–13 and $Kn = 0.01$–0.09) as measured by Legge and Koppenwaller.[103] The adequacy of the cell size and the DSMC capability for describing unsteady separation in this near-continuum range deserves further study.

DSMC calculations and experiments on plume-freestream interaction have been made by Campbell[104]; a comparison of the density distribution shows qualitative agreement. A three-dimensional version of DSMC calculations for a delta wing[105] are compared with a Deutsch Forschungsanstalt für Luft–und Raumfahrt windtunnel experiment at Mach 8.9 and Knudsen numbers of 0.02–2.0. Good agreement is found for the lift, drag, and surface heating rate. However, the surface temperature is believed to be near the freestream stagnation value in this case. The aerodynamics of a viscous optimized waverider in the rarefied gasdynamics regime is examined with DSMC calculations by Rault.[106] With the F3 program of Bird,[107,108] Rault obtained an L/D of 0.24 at Mach 25 and 100-km altitude ($Kn = 0.01$). It is seen to be inferior to the aforementioned delta wing, which has an L/D better than 0.5 even at a Kn as large as 0.10. Interestingly, a three-dimensional DSMC calculation made for the very blunt AFE configuration[109] gave an $L/D = 0.212$ at 100 km, not far from Rault's value of 0.24. Of course, at Mach 25 and 100-km altitude, any vehicle needs little lift since the large centrifugal force developed means that the vehicle is nearly in a low-Earth orbit.

A more critical assessment of the DSMC method is to sample the velocity-distribution function $f(u, v, w)$ and compare this with corresponding experimental data. Several sets of unpublished data for argon and helium, ideal for this purpose, have been previously obtained by E. P. Muntz for the partially integrated f within the shock-transition zone. This result is deduced from measured intensity profiles of predominantly Doppler-broadened emission lines excited by an electron beam, known as the electron fluorescence technique. Difficulties are encountered, however, in identifying the precise location at which each measurement is made, owing to a number of uncertainties related to the instrument and to the flowfield nonuniformity. Comparison studies[110–112] thus serve as validation of the experimental procedure as well, especially since a convolving calculation procedure is adopted in some cases to identify the location that best fits a particular experimentally determined (parallel or perpendicular) distribution function. In their analysis, Erwin et al.[110] use differential cross sections based on a Maitland et al.[13] potential, in place of the VHS collision model, that fits experimental viscosity data slightly better than other forms.

Two sets of predicted and experimentally deduced velocity distribution functions for a Mach 25 shock in helium are reproduced from Pham-Van-Diep et al.[111] and are shown in Fig. 3. The convolved parallel and perpendicular distributions

$$f_\parallel(u) = \iint f \, dv \, dw, \qquad f_\perp(v) = \iint f \, du \, dw$$

are drawn as solid and dashed curves, respectively, with the corresponding experimental data shown as open circles and open triangles. The data set of Fig. 3a are identified with a spatial location where the number density ratio $\tilde{n} \equiv (n - n_1)/(n_2 - n_1)$ is 0.285, whereas the set of Fig. 3b is for a further downstream station where $\tilde{n} = 0.565$. Similarly detailed agreement is found with helium at $M_\infty = 1.59$ and argon at 7.18.[110] These close comparisons indicate the remarkable ability of DSMC to predict the population of scattered atoms in a highly nonequilibrium state. They unmistakably reveal the Mott-Smith[114] type of bimodal distribution for $f_\parallel$, which signifies the persistent influence of the upstream and downstream states. It remains to be seen if the VHS version of the DSMC can also produce a similarly encouraging comparison. (A limited study with VHS indicated general agreement with noticeable differences only in the vicinity of the $f_\parallel$ maximum.[115])

Here again, the possibility of a localized, weak unsteadiness (on the upstream side of the shock structure) has not been examined and is lost in the long-time averaging required by the model procedure. Time-accurate results, however, from DSMC calculations require greater computer resources and care in programming. An example of such DSMC solutions for a transient thermal heating problem in one spatial dimension[116,117] appears to be encouraging.

Continuum Extension to Rarefied Hypersonic Flows

The foregoing discussion demonstrates that the DSMC method can treat problems normally handled by NS-based equations, but it demands large and costly computer resources. For example, one of the Carlson and Wilmoth[100] DSMC calculations took 33 days on a dedicated Sun SPARC station-2, and the three-dimensional calculation of Celenligil et al.[109] needed 35 CPU hours on a CRAY-2. NS-based solutions have proven useful in low-density hypersonic flow studies[118,119] and compare reasonably well with surface heat flux measurements in hypersonic flows.[120,121] With DSMC calculations, it becomes possible to assess the NS-based results and other continuum extensions and identify their applicability domains. This is accomplished, in part, by Moss and Bird,[122] Gupta and Simmonds,[123] Moss et al.,[124] and subsequent workers, by comparing DSMC, NS, and NS-based VSL calculations for a blunt-nose flow region. The following discussion examines recent works on kinetic theory based extensions of the continuum model. Several concepts used in the discussion first need to be clarified.

Just as with the inviscid shock layer in the classical theory, the concept of a thin shock layer may be applied to the viscous, heat conducting flow region between the shock and the surface of a blunt

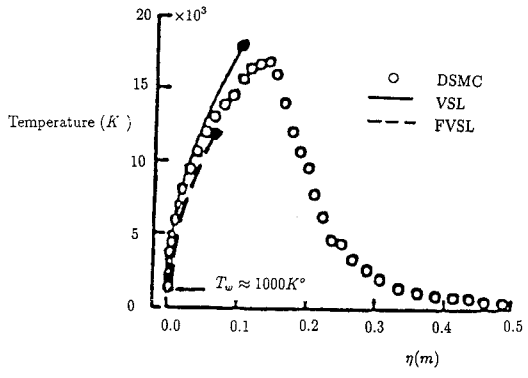

a)

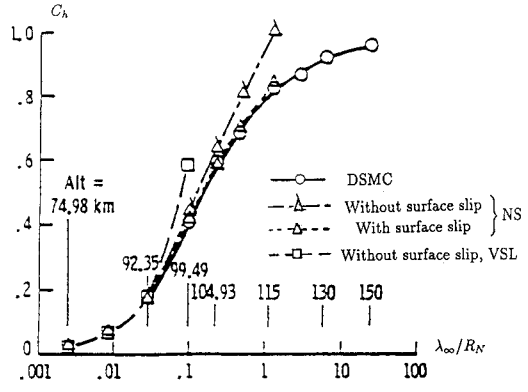

b)

Fig. 4 Comparisons of DSMC, VSL, FVSL, and NS calculations. a) The temperature distribution along the stagnation streamline when R_N = 1.3 m, U_∞ = 7.5 km/s, an altitude of 92 km, $T_w \cong 10^2 K$, and the surface is noncatalytic (from Moss and Bird[122]). b) The surface heat transfer coefficient as a function of the Knudsen number when U_∞ = 7.2–7.5 km/s and the altitude range is 75–115 km (from Gupta and Simmonds[123]).

or nonslender body, provided the density level in the layer is much higher than that in the freestream. Viscous formulations based on a thin shock-layer approximation could be referred to as a viscous shock-layer theory. A distinction, however, must be made between a version that uses the viscous modified Rankine–Hugoniot relations at the outer boundary and one that assumes inviscid shock relations. The latter version has been called VSL by Moss and Bird[122] and Moss et al.[124] The version with the viscous modified shock conditions will be referred to as a *fully* viscous shock layer (FVSL) to avoid unnecessary confusion. The FVSL version of the NS equations and its extension has served as the main analytical vehicle in the former Soviet Union with which much of their nonequilibrium high-temperature flow physics and three-dimensional studies were carried out.[5,125]

Because of its resemblance to wall slip, the change in shock boundary conditions in the FVSL formulation, which includes corrections to the tangential velocity and total enthalpy, is called *shock slip* by Davis,[126] Moss, and others. Underlying these modified shock conditions is the stipulation that the density in the interior of the shock is low and comparable to the freestream level. Consequently, the tangential components of the mass, momentum, and energy fluxes have little effect on the balances in the normal flux components, as long as the thickness of the shock is small compared with the shock or body radiuses of curvature (even if the shock thickness becomes comparable to the thickness of the shock layer[119,127]). This implies that a shock-capturing NS solution should provide the shock slips correctly, even when the structure of the shock is not physically correct on a kinetic theory basis. A FVSL formulation may therefore provide a framework where a kinetic theory basis for a continuum extension can be found.

Examples assuming a surface with a low wall-to-stagnation temperature ratio ($T_w/T_0 \ll 1$) are more relevant to hypersonic flight than an example with a nearly insulated wall. Strong wall cooling also makes the thin shock-layer analyses a better approximation for FVSL, since the shock-layer density level is raised substantially. An additional consequence of strong wall cooling is to restrict the wall-slip influence of the FVSL and VSL formulations to a relative order of $(\epsilon T_w/T_0)^{\frac{1}{2}}$,[119,127] where ϵ is the small parameter in the shock-layer theory and denotes the ratio of the freestream density to a typical shock-layer density.

We shall provide examples where the degree and manner of the various NS-based predictions differ from one another and from DSMC calculations in the low-density regime of interest. Figure 4a, reproduced from Moss and Bird,[122] shows a comparison for the temperature along the stagnation streamline when the blunt nose, with a radius of 1.3 m, is highly cooled and noncatalytic. The VSL prediction (solid line) provides a noticeably larger effective temperature than the DSMC data (circles) at the outer part of the shock layer. To examine shock-slip effects, a corresponding FVSL profile,[118,119] with a binary reacting gas model, is shown as a dashed curve. The viscous and heat conduction corrections at the other edge decrease the temperature in the outer portion of the FVSL and reduce its thickness. This figure also illustrates the extent of the DSMC shock structure in this type of flow; it is almost twice the shock-layer thickness. However, owing to a lower density level, its direct influence on the downstream flow is limited.

Figure 4b, reproduced from Gupta and Simmond,[123] shows a comparison of the stagnation point heat transfer coefficient C_h over a wide range of Knudsen numbers for a nose radius of about 1.36 m. The VSL solution (squares), without wall slip, begins to depart from the DSMC solution (circles) above $Kn \cong 0.025$. The NS solution without wall slip (triangles) remains close to the DSMC solution up to $Kn \cong 0.25$, where shock-slip effects become significant. With wall slip, the shock-capturing NS solution, which automatically accounts for shock-slip effects, agrees surprisingly well with DSMC all of the way up to $Kn = 1$. However, in a similar study by Lee et al.,[128] this version of the NS solution reaches the $C_h = 1$ limit at $Kn \cong 2.5$ and suggests a peculiar trend of overshooting the limit when $Kn \geq 2.5$. In a subsequent report on stagnation-point heating predictions at AFE conditions, Gupta et al.[129] found that wall-slip effects are not significant in both the NS and VSL calculations. The discrepancy between the VSL and NS results in the low-Reynolds-number-range (Figs. 6–10 in Ref. 129) indicates clearly the importance of shock-slip effects that are unaccounted for in their VSL model. In fact, their NS results closely reproduce the FVSL calculation of Cheng[127] when correlated with his K^2 parameter.

Kinetic Theory Basis for NS, Burnett, and the 13-Moment Equations

Early research was not successful for the improvement of the NS description for rarefied flows by applying the 13-moment equations of Burnett[130] or Grad.[131] The general belief was that these higher order equations from kinetic theory are not able to predict when the NS relations break down.[132] This perception apparently has changed as a result of recent CFD and DSMC calculations, notably the study of plane shock structure by Fiscko and Chapman.[133,134]

The theoretical basis of the NS and Burnett equations is the formalism of the Chapman–Enskog expansion and the successive development for the velocity distribution function under the assumption that the particle collision time, λ/c (where c is the thermal speed) or μ/p, is small compared with a flow characteristic time.[72,135–137] More precisely, the requirements are

$$\left|\frac{p_{ij}}{p}\right| \ll 1, \qquad \left|\frac{q_i}{pc}\right| \ll 1, \qquad (i, j = 1, 2, 3)$$

where p_{ij} is a component of the deviatorical pressure tensor, and q_i is a component of the thermal heat flux.

The Burnett equations, as well as the extension to the *super-Burnett* equations,[138] are, therefore, strictly valid only as successive corrections to the Euler equations appropriate to a nearly *inviscid* flow (outside of boundary and shear layers). This is because inviscid/isentropic relations were used to simplify the Dp_{ij}/Dt and Dq_i/Dt substantial derivative terms in the final form of the constitutive relations. Hence, these relations are not valid in either a fully viscous region or a boundary layer. The formulation is more restric-

tive than merely requiring that $|p_{ij}/p|$ be small. This requirement makes the (standard) practice of solving the full Burnett equations, with all terms treated as equally important, conceptually difficult. Together with this is the unresolved issue of proper boundary conditions. As Schaaf and Chambré[132] noted, if the Burnett system is to be solved fully, terms of an order higher in the derivatives occur in the equations, and additional boundary conditions must be prescribed. Thus, a nonuniqueness problem arises unless the system possesses some special property as occurs in shock structure studies, where a wall is not present. This issue cannot be settled by simply demonstrating the existence of a solution. Objection to the Burnett equations has also been raised concerning its loss of frame invariance when applied to a rotating system.[139]

Grad's system of 13-moment equations is a particular set of velocity moments of the Boltzmann equation, i.e., the Maxwell transfer equations in which closure is achieved with the help of an assumed form of the distribution function

$$f = \rho\left(\frac{\beta}{\pi}\right)^{3/2} e^{-\beta c^2}\left[1 + A_{ij}c_ic_j + B_ic_i + C_ic^2c_i\right] \qquad (8)$$

where $\beta = (2RT)^{-1}$, c_i is a thermal velocity component, and $c^2 = c_1^2 + c_2^2 + c_3^2$. The polynomial coefficients can be identified with stress-tensor and heat flux components as

$$A_{ij} = \frac{p_{ij}}{2pRT}, \qquad B_i = -\frac{q_i}{pRT}, \qquad C_i = \frac{q_i}{pRT}\,\frac{1}{5RT}$$

The quantity inside the square brackets of Eq. (8) is a truncated Hermite polynomial expansion carried out for the 20th moment in Grad's original work.[131] Equation (8) turns out to be precisely the form needed for f in the Chapman–Enskog theory for the derivation of the NS and Fourier constitutive relations and the evaluation of the viscosity and heat conductivity coefficients. The various p_{ij} are symmetric; hence, the p_{ij}, q_i, u_i, and ρ are 13 unknowns in the partial differential equations of the 13-moment system. These equations do not require that μ/p or $Kn = \lambda/L$ be small, as long as Eq. (8) remains adequate. More specifically, this amounts to allowing nonvanishing values for

$$p_{ij}/p,\ q_i/(2RT)^{\frac{1}{2}} = 0(1) \qquad (9)$$

Surprisingly, the full Burnett equations, including the usual boundary conditions for velocity and temperature, turn out to be derivable from Grad's 13-moment equations in the case of a Maxwell gas for asymptotically small μ/p or $|p_{ij}/p|$; this is noted by Schaaf and Chambré[132] and more explicitly by Yang.[140] To be sure, Burnett's original theory actually involves a form far more complicated and pertains to an order higher than that in Eq. (8). The corrections for a non-Maxwell monatomic gas in both the Burnett and 13-moment equations are believed to be rather small.[133,135,140] For application to supersonic flows, the 13-moment equations fail to yield a normal shock structure when $M_\infty > 1.65$, as is well known.[141] Consequently, the system, without modification, cannot provide a foundation for the entire flowfield that includes the shock structure. We later examine its applicability to the flow behind a shock.

Burnett Equations as a CFD Model for Rarefied Hypersonic Flows

Navier–Stokes calculations are known to give inaccurate shock-structure descriptions when compared with results from particle simulation methods and experimental results.[73,74,132] In fact, Garen et al.[142] show poor agreement between a Mach 1.06 shock structure in argon and a corresponding NS solution. With a time-dependent, flux-splitting technique, Fiscko and Chapman[133,134] found that the Burnett equations provide greater accuracy than the NS equations for one-dimensional shock structure in a monatomic gas. The degree of improvement over NS varies, however, depending on the Mach number, the viscosity-temperature law, and especially the flow quantities of interest. The encouraging agreement with particle simulation results demonstrated in Refs. 133 and 134 suggest that a CFD model based on the Burnett equations may provide a much improved shock-capturing capability relative to NS, for a rarefied hypersonic flow, where a realistic description of the shock structure at a high temperature would be of vital aerothermodynamic interest. Apart from the issue of surface boundary conditions, there is another obstacle to this extension, first noted by Bobylev[143] and Foch.[144] Namely, the numerical solution is linearly unstable to disturbances with wave lengths comparable to, or less than, the mean free path, and this difficulty is believed to place a handicap on Fiscko and Chapman's[133,134] time-dependent calculations. Zhong et al.[145,146] overcame this problem by adding several higher order derivative terms to the Burnett constitutive equations. These added terms have forms similar to certain terms at the super-Burnett level but with different coefficients (and signs). The *augmented-Burnett* constitutive equations for the deviatorial stress and heat-flux components are written as

$$\sigma_{ij} = \sigma_{ij}^{(1)} + \sigma_{ij}^{(2)} + \sigma_{ij}^{(a)}, \qquad q_i = q_i^{(1)} + q_i^{(2)} + q_i^{(a)}$$

where the (1) and (2) superscripts, respectively, refer to the NS and Burnett levels, and an (a) indicates the added terms. In the one-dimensional case, e.g., $\sigma_{11}^{(2)}$ and $q_1^{(2)}$ contain terms such as

$$\sigma_{11}^{(2)} = \frac{\mu^2}{p}\left(\alpha_1 u_x^2 + \alpha_7 RT_{xx} + \alpha_9\frac{RT}{\rho}\rho_{xx} + \cdots\right)$$

$$q_1^{(2)} = \frac{\mu^2}{p}\left(\gamma_1\frac{T_xu_x}{T} + \gamma_3 u_{xx} + \cdots\right)$$

and the added terms are

$$\sigma_{11}^{(a)} = \frac{\mu^3}{p^2}\omega_7 RTu_{xxx}$$

$$q_1^{(a)} = \frac{\mu^3}{p\rho}\left[\theta_7 RT_{xxx} + \theta_6\frac{RT}{\rho}\rho_{xxx}\right]$$

The arbitrary values for the coefficients are taken to be $\omega_7 = 2/9$, $\theta_6 = -5/8$, and $\theta_7 = 11/16$ in the numerical study by Zhong et al.[145] These terms, nevertheless, stabilize the Burnett equations. Incidentally, this set may be compared with that in Ref. 147 for a Maxwell gas, which gives $\theta_7 = -157/116 \neq 11/16$. In several cases, the augmented-Burnett results provide improved accuracy over Fiscko and Chapman's earlier version.

Of engineering interest are the two-dimensional examples in Zhong et al.[145,146] that compare the NS, augmented-Burnett, and particle simulation calculations. They are among the first Burnett solutions to a hypersonic blunt-body problem to appear, and for which the boundary condition issue must be addressed. The (M_∞, Kn) pairs considered are (4, 6.7×10^{-5}), (10, 0.10), (10, 1.2), and (25, 0.28), and are, respectively, referred to as cases I–IV. A constant specific heat ratio $\gamma = 1.40$ is assumed, except in case IV, where rotational relaxation is allowed in both the Burnett and the particle simulations. However, the surface temperature assumed is not low, being in the T_w/T_0 range of $\frac{1}{3}$ to $\frac{1}{2}$. Here, the Burnett and NS solutions share the same wall-slip boundary conditions, whereas the corresponding surface conditions for the particle simulation calculation were not explained. Density and temperature distributions along the stagnation streamline were obtained and compared for cases II, III, and IV, where the differences among the three solution sets are seen to be small, especially in the density profiles. In these examples, even in the interior of a thick shock, where discrepancies of the NS temperature predictions are noticeable, the NS solution actually describes the temperature profile fairly well. This is in contrast to the more drastic differences between NS and Burnett shock structures found in earlier studies.[89,133,134]

Figure 5, from Zhong et al.,[145] compares the density and temperature profiles for case IV, where the temperature profiles of the three solutions sets are seen to be indistinguishable from one another inside the shock layer, including near the body. This is surprising because the FVSL parameter K^2 for this case is of order unity,[119] which signifies a large departure from translational equilibrium. This result could have stemmed from the assumed Sutherland viscosity law or from the particular iterative procedure used, which avoids additional boundary conditions by extrapolating from the

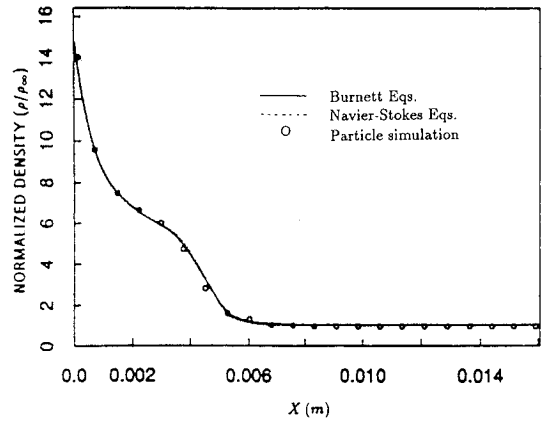

a)

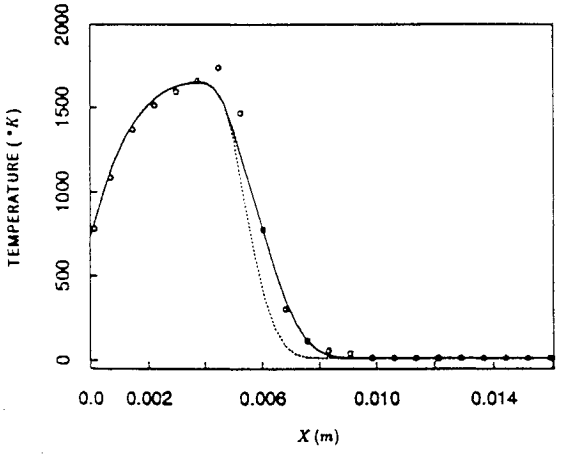

b)

Fig. 5 Comparison along the stagnation streamline of the augmented-Burnett, NS, and particle simulation calculations for case IV with M_∞ = 25, Kn = 0.28, and K^2 = 0.95 (from Zhong et al.[145]): a) density and b) translational temperature.

interior of the layer to the wall. The study shows that the Burnett equations in this case can yield a solution that closely matches the particle-simulation results. On the other hand, this comparison also indicates that NS calculations can predict the shock and flow structures almost as well as the Burnett formulation. This CFD study, however, falls short in settling the uniqueness issue, which cannot be answered by simply demonstrating a solution's existence. For steady Couette flow, Lee[148] shows conclusively that, even with such an extrapolation technique, the numerical solution is not unique and depends on the initial input for the iteration.

In a subsequent study, Zhong[149] proposed a set of additional wall boundary conditions that render the numerical solution unique. This is accomplished by assigning the normal gradient of the tangential stress at the wall its NS value, which amounts to Schamberg's[150] more systematic derivation of the wall-slip conditions, thereby departing from the original intent of fully solving the nonlinear Burnett system. A comparison with a DSMC solution for an aligned flat plate with $Kn = 0.20$ shows the scheme is ineffective, since a discrepancy comparable to that found with the corresponding NS solution results.

Thirteen-Moment Equations as a Basis for FVSL Theory

As noted earlier, the use of FVSL and VSL, as well as the full NS equations in rarefied hypersonic flow analyses, anticipates that viscous and other molecular transport effects rank equally with convective processes, which also implies conditions (9). The same conditions indicate, however, a large departure from translational equilibrium, invalidating the gas-kinetic basis for the NS and the Burnett equations. Grad's 13-moment theory, which allows conditions (9), may therefore serve as a kinetic theory basis for a viscous shock-layer analysis. Another reason for using the 13-moment equations is the absence of ambiguity in the type and number of admissible boundary conditions at a body surface. By considering the number of characteristics reaching the boundary, Grad[131] showed that the number and type of needed boundary conditions are the same as for the NS equations. This is also confirmed by examining the nature of the 13-moment equations in a Couette flow.[151] With scales typical of flow in a shock layer, it is possible to express the order of magnitude of $|p_{ij}/p|$ explicitly in the form of the reciprocal of a local Reynolds number

$$\bar{x} = \epsilon \frac{p_\infty U_\infty x}{\mu_0} \left(\frac{\mu_0}{\mu_*} \frac{T_*}{T_0} \right) \sec \beta_* \tag{10}$$

where β_* is the shock or body incidence angle, the asterisk subscript refers to a suitable reference condition, and x is a distance measured from the origin. With x replaced by the nose radius R_N, $\bar{x}$ is identified with the K^2 parameter in Cheng's[119,127] early NS-based theory. Thus, $\bar{x}$ or K^2 controls both the shock slip and departure from translational equilibrium. The Knudsen number $Kn = \lambda_\infty/L$ and $V \equiv \chi/M_\infty^2$, commonly used in rarefied gasdynamics, are related to $\bar{x}$ as

$$Kn \sim 2 \left(\epsilon \frac{T_*}{T_0} \right)^{\frac{1}{2}} (\bar{x})^{-1}, \qquad V \sim (\bar{x} \cos \beta)^{-\frac{1}{2}} \tag{11}$$

With scales appropriate for the shock transition zone, a thin-layer approximation can be applied to derive the equations governing the quasi-one-dimensional interior of the shock. They can be integrated to arrive at the modified Rankine–Hugoniot relations that involve the shear stress and heat flux contributions immediately behind the shock, which are identified as shock slips. We utilize a conventional notation, with y and v referring to the coordinate and velocity components in the direction normal to the body surface. The shock slip conditions are

$$u - u_\infty = p_{12}/m_1, \qquad w - w_1 = p_{32}/m_1$$

$$H - H_\infty = (up_{12} + wp_{32} + q_2)/m_1$$

where $m_1 = \rho_\infty v_1$ represents the component of the freestream velocity normal to the surface, q_2 is the normal heat flux component, and p_{12} and p_{32} are pressure-tensor components associated with the (x, y) and (z, y) planes, respectively. These relations are subject to an error of order ϵ; they provide the outer boundary conditions for the shock-layer flow, irrespective of the gas-kinetic model used for the shock's interior.[152] The remaining shock condition is $P_{22} = m_1 v_1$, where the normal pressure-tensor component $P_{22}(= p + p_{22})$ is not the thermodynamic pressure p, owing to translational nonequilibrium.

The governing equations for the shock-layer flow behind the shock are, to leading order, essentially the same as in the VSL or FVSL theories, except that the constitutive relations expressing p_{12}, p_{32}, p_{22}, and q_2 in terms of flow gradients are replaced with those given by the 13-moment theory. Under the thin-layer approximation and with the formalism of a small ϵ familiar from shock-layer theory, i.e., consider R/c_p to be 2ϵ, the constitutive relations in question can be reduced to[151,152]

$$p_{12} = -\frac{P_{22}}{p} \mu \frac{\partial u}{\partial y} \tag{12a}$$

$$p_{32} = -\frac{P_{22}}{p} \mu \frac{\partial w}{\partial y} \tag{12b}$$

$$q_2 = -\frac{P_{22}}{p} k \frac{\partial T}{\partial y} \tag{12c}$$

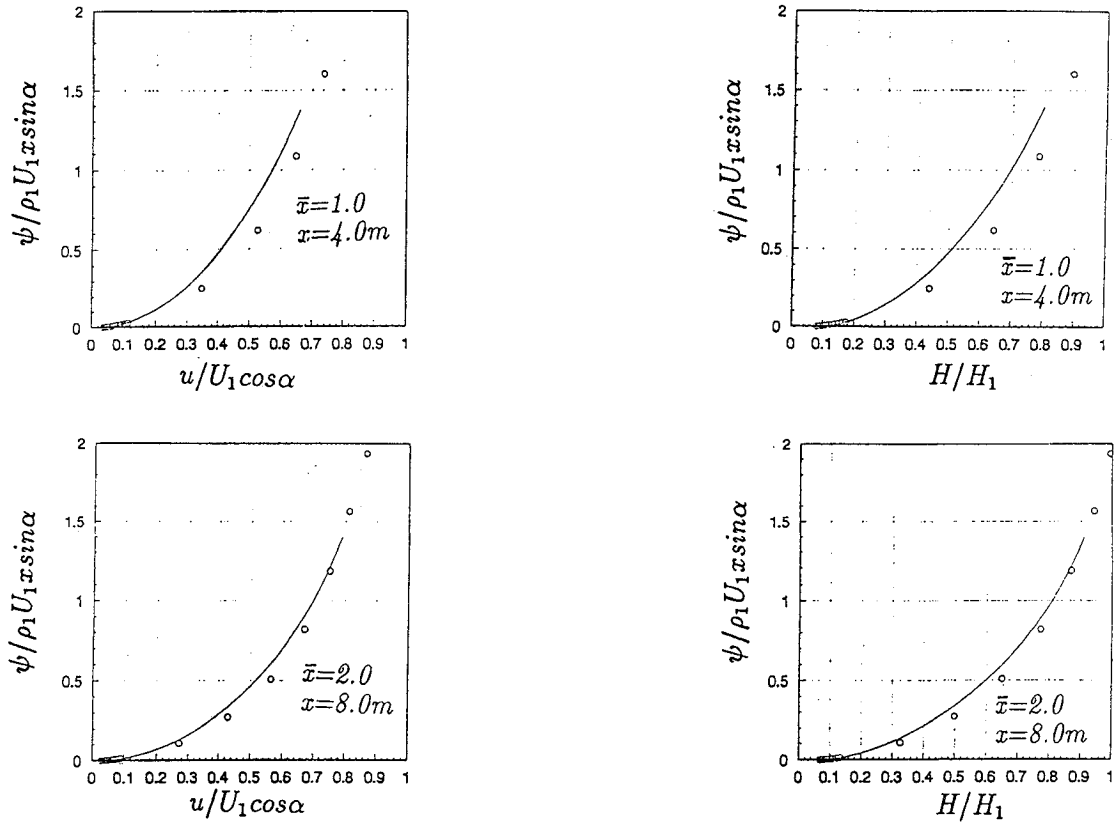

Fig. 6 Comparison of the tangential velocity and total enthalpy between the 13-moment based FVSL and DSMC results vs a dimensionless stream function $\bar{\psi}(=\psi/\rho_1 U_1 x \sin\alpha)$ (from Wong[155]). A Maxwell gas flows over a flat plate at 20-deg incidence with M_∞ = 24.6. The small circles are the DSMC results whereas the solid line is the FVSL result.

where

$$\frac{p}{P_{22}} = 1 + \frac{2}{3}\left(\frac{\mu}{p}\frac{\partial u}{\partial y}\right)^2 + \frac{2}{3}\left(\frac{\mu}{p}\frac{\partial w}{\partial y}\right)^2 - \frac{4}{3}\frac{R}{Pr}\frac{1}{P_{22}}\frac{\mu}{p}\frac{\partial}{\partial y}\left(P_{22}\frac{\mu}{p}\frac{\partial T}{\partial y}\right) \tag{12d}$$

The previous expressions differ from the corresponding NS relations mainly in the appearance of the common factor P_{22}/p, which is determined by a nonlinear relation, Eq. (12d). It is, in fact, through p, not P_{22}, that translational nonequilibrium alters the dynamics and thermodynamics of a viscous shock layer. Except for the rightmost term of the last equation, the previous constitutive relations involve derivatives of u and T no higher than first order and differ from those in the Burnett theory. The last term in Eq. (12d) is a higher order contribution identified as a thermal stress[72] and is included because of its relatively large coefficient and interesting physical significance. To complete the formulation, we apply wall-slip equations from Grad's wall model, suitably simplified in a manner consistent with Eqs. (11) and (12). These wall-slip effects, however, can influence the shock flow, at most to the relative order $(\epsilon T_w/T_0)^{\frac{1}{2}}$, as indicated earlier. Wall-slip effects have been demonstrated to be negligibly small, even for exceptionally large accommodation coefficients.[153]

The previous observation about the nonequilibrium influence through the P_{22}/p ratio indicates the possibility of correlating a kinetic-based shock-layer flow with a NS-based flow. A key observation is the recognition that the reciprocal of the density ρ, or of p, always appears in a product together with a normal $\partial/\partial y$ derivative, both in the governing differential equations and in the outer boundary conditions that involve shock slip. The ϵ or p may then be eliminated with the use of Dorodnitsyn or von Mises variables. The governing equation system is thus transformed to a NS-based system, with slightly different wall-slip boundary conditions. The latter is inconsequential for the strongly cooled surface of interest. This correlation principle holds for the tangential velocity components and the enthalpy, and, consequently, for the temperature, the major stress components p_{12} and p_{23}, and the heat flux q_2. A consequence is that the skin friction and surface heating rate are predictable from the NS-based equations. They are unaffected by translational nonequilibrium, to leading order, although the streamline pattern and shock-layer thickness are accordingly displaced. This version of the theory therefore provides a kinetic theory basis for explaining the rather good agreement of the NS-based FVSL analyses with heat transfer measurements discussed earlier for low-density hypersonic flows.[118,119] It was called to the authors' attention that a thin-layer version of the constitutive relations, similar to Eqs. (12), had been derived from the 13-moment equations by Kuznetsov and Kikol'skii,[154] but their development stops short in recognizing the correlation principle that allows a unique connection to NS solutions and that is the main concern here.

Figure 6, reproduced from Wong,[155] compares the DSMC and FVSL solutions for the velocity and total enthalpy profiles in a shock layer over a 10-m-long, flat, windward surface at an incidence of α = 20 deg, where dimensionless von Mises variables $(\bar{\psi}, \bar{x})$ are utilized. The study assumes the flow of a Maxwell gas at M_∞ = 24.6, a chord Reynolds number Re_∞ = 300/m, a speed of 7.5 km/s at an ambient temperature and density of a standard atmosphere at 100 km, and a highly cooled surface with $T_w/T_0 \cong 0.036$. Results are shown at two x stations, where $\bar{x}$ = 1 and 2. In spite of the parameter ϵ equalling $\frac{1}{4}$ for a monatomic gas, the comparison shows reasonable agreement with, and substantiates, the correlation principle. With this principle, the nonequilibrium profiles vs a dimensionless $\bar{y}$ coordinate can be predicted with similar success. Cases are compared at incidence angles of 30 and 40 deg with comparable results, although the 40-deg case is less satisfactory because of the failure of the FVSL description near the leading edge, which causes an appreciable discrepancy in the downstream shock layer.

Wong's[155] study confirms the important dimensionless variables $\bar{x}$ and P_{22}/p [see Eqs. (10) and (12d)] that control the FVSL fluid dynamics. Although P_{22}/p is expected to approach unity far downstream, where $\bar{x} \to \infty$, there also exists an $\bar{x}$ range of unit order where this parameter remains quite close to unity. In this case,

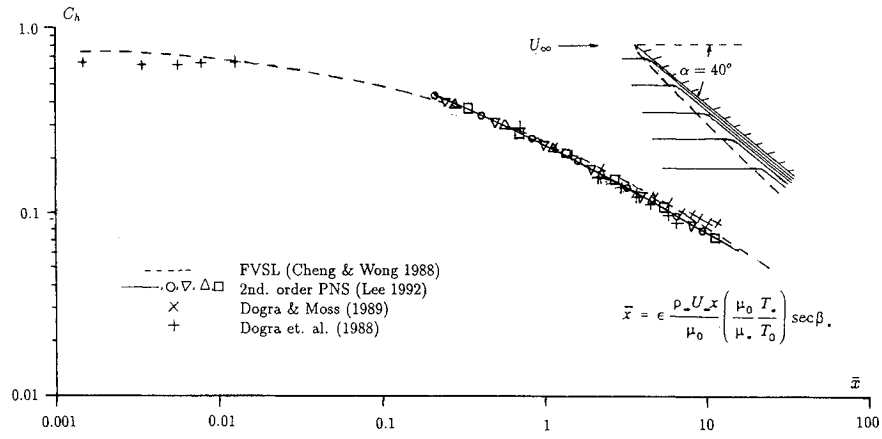

Fig. 7 Correlation of DSMC and NS-based calculations with the FSVL analysis for the surface heating rate on the compression side of a flat plate as a function of a rescaled Reynolds number $\bar{x}$, given by Eq. (10). The plate is at a 40-deg incidence angle, is highly cooled ($T_w/T_0 \cong 0.04$), $U_\infty = 7.5$ km/s, and is in a standard atmosphere.

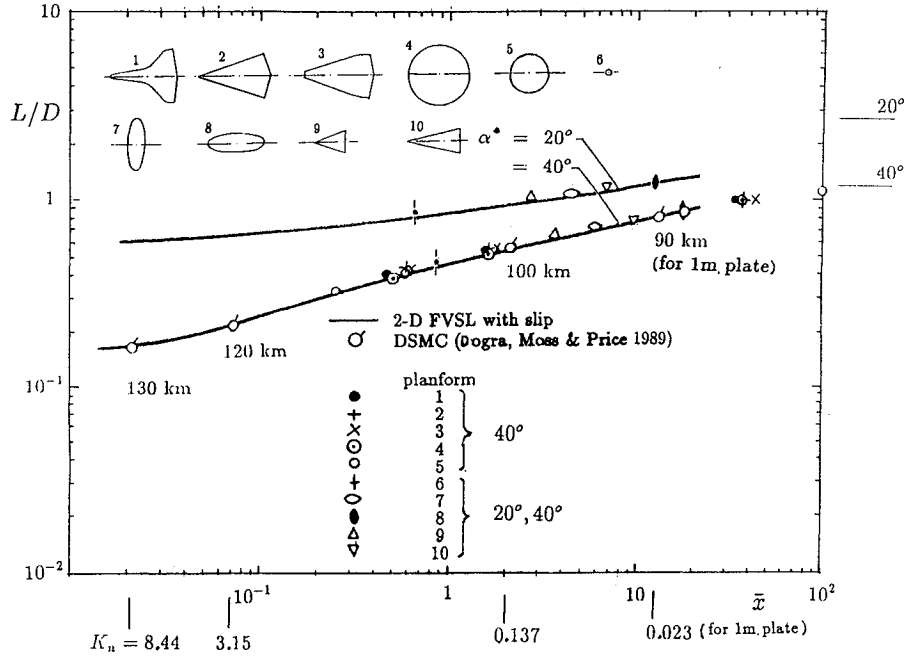

Fig. 8 Correlation of the lift-to-drag ratio of planar lifting surfaces at a 40-deg incidence angle in a standard atmosphere for two-dimensional FVSL, DSMC, and three-dimensional FVSL results as a function of $\bar{x}$. The symbols are for 10 planforms computed by a strip method based on three-dimensional FVSL theory in which the span-averaged chord varies from 0.47 to 19.19 m.

the physical structure of the entire shock layer is unaffected by a large departure from translational equilibrium, to within an error of $0(\epsilon)$.[155]

Cheng et al.[151,152,156] (also see Cheng[157]) studied the generic lifting surface problem of a flat plate at an attack angle of 40 deg in a rarefied hypersonic flow. Solutions based on FVSL, parabolized (thin-layer) NS, and time-accurate NS calculations are compared with corresponding DSMC computations.[102,158] Examples include a monatomic Maxwell gas and a diatomic gas model with $\gamma = 1.40$ and $Pr = 0.72$ (which implies a fast rotation-translation energy transfer), and cases with different viscosity-temperature relations, wall temperatures, and wall-slip models. Although some of the DSMC air data are generated from a code that allows internal excitation and chemical reactions, the latter effects on aerothermodynamics are negligible even at a flow speed of 7.5 km/s, because of the high degree of gas rarefaction at altitudes of 90–130 km. The coefficients of heat transfer and skin friction, C_h and C_f, from three sets of DSMC data and six sets of NS-based results, each with different M_∞, Re, and viscosity laws, are determined over a wide range, 0.2–10, of $\bar{x}$. The range increases to 10^{-3} through 10 if the DSMC data near the collision-free limit are included. Figure 7 presents the C_h correlation as a function of $\bar{x}$. Even though a perfect Reynolds analogy is not expected, the corresponding correlation for C_f turns out to be almost indistinguishable from that in Fig. 7, except for a portion of the DSMC calculation at a 100-km altitude, which defies explanation.

The lift-to-drag ratio of a plate at 40-deg incidence is computed from the integrated normal and tangential forces on the windward side and are reproduced in Fig. 8 from Cheng et al.[152] The two-dimensional FVSL results (solid curves) agree exceedingly well with the Dogra and Moss[158] DSMC calculations for a 1-meter plate (in open circles with slashes) over the entire $\bar{x}$ range (2×10^{-2} through 15). Also included as a solid curve is the L/D computed for a plate at a 20-deg angle of attack. Of interest are L/D values computed for 10 widely different planforms based on the two-dimensional distributions of skin friction and normal force (reproduced from Cheng[159]). These calculations use a version of the strip method, which is a result of the three-dimensional FVSL theory for a flat-bottomed surface.[152,156] When the distance x in the two-dimensional problems is taken to be the span-averaged chord, the

10 L/D values fall in the vicinity of the strictly two-dimensional results. This is surprising because, as altitude or Knudsen number increases, the planform shape is expected to strongly affect the skin friction, hence the L/D. This insensitivity of the L/D on planform shape indicates a way to identify the bridging function for planar lifting surfaces,[75,160–162] which is provided here by the two-dimensional data for an inclined plate.

The thin-layer version of the constitutive relations, Eqs. (12), may also be adapted to convert the parabolized NS system, discussed in Ref. 1, to rarefied flow applications. The flows over an aligned flat plate and on the lee side of a flat surface, where the rarefaction is extreme, remain as examples from which still more can be learned from a critical comparison of continuum-extension and particle-simulation calculations.

Concluding Remarks

This Survey discusses two related major areas of hypersonic flow research. Both topic areas are central to the study of highly nonequilibrium flow physics and aerothermodynamics that are important in atmospheric re-entry and for sustained hypersonic flight. The basic physics and fluid dynamics, however, are also important in other areas that are not discussed, such as scramjet engines and ram accelerators.

The first topic focused on the description of the internal state of diatomics, particularly air or its reactive derivatives. Although significant progress has been made in recent years, uncertainty still remains in modeling the intermolecular and internuclear potentials as well as inelastic collisions. Radiative processes are also still uncertain. These difficulties remain as obstacles to adequate quantitative predictions of heat transfer and skin friction. As has been pointed out, the internal states at high temperature not only significantly affect the internal energy of the flow but may have additional "real-gas" effects, such as altering the transport properties. These effects, in turn, make the high-temperature prediction of flow instability and turbulence transition uncertain.

Progress has been made in the modeling of viscous, rarefied hypersonic flow, which also involves a significant degree of translational nonequilibrium. At sufficiently high relative speeds, the gas may be chemically reactive and possess nonequilibrium internal modes, as many DSMC air calculations have indicated. Again, there is no shortage of unresolved critical issues involving nonequilibrium flow physics and their modeling strategies.

The pace of progress in both topic areas is limited, to a large extent, by the difficulty in obtaining experimental data. Here, too, progress is being made in high-enthalpy flow simulations,[9,163,164] as well as nonequilibrium gas-state diagnostics in low-density hypersonic flows.[9,97,98]

Acknowledgments

This study was supported by the NASA/DOD Grant NAGW-1061 and by the Air Force Office of Scientific Research Math Information Science Program for the part by the first author. Many individuals have helped the authors in one way or another during the course of this review; among them are V. K. Dogra, A. Hertzberg, J. A. Kunc, C. J. Lee, T. C. Lin, J. N. Moss, E. P. Muntz, C. Park, G. C. Pham-Van-Diep, J. W. Rich, C. E. Treanor, P. L. Varghese, D. Wadsworth, D. Weaver, E. Y. Wong, H. T. Yang, and X. L. Zhong.

References

[1]Anderson, J. D., Jr., *Hypersonic and High Temperature Gas Dynamics*, McGraw–Hill, New York, 1989.

[2]Park, C., *Nonequilibrium Hypersonic Aerothermodynamics*, Wiley, New York, 1990.

[3]Cheng, H. K., "Perspectives on Hypersonic Viscous and Nonequilibrium Hypersonic Flow Research," Univ. of Southern California, Dept. of Aerospace Engineering, Rept. USCAE 151, Los Angeles, CA, 1992.

[4]Cheng, H. K., "Perspectives on Hypersonic Viscous Flow Research," *Annual Review of Fluid Mechanics*, Vol. 25, 1993, pp. 455–484.

[5]Tirsky, G. A., "Up-to-Date Gasdynamic Models of Hypersonic Aerodynamics and Heat Transfer with Real Gas Properties," *Annual Review of Fluid Mechanics*, Vol. 25, 1993, pp. 151–181.

[6]Billig, F. S., "Research on Supersonic Combustion," AIAA Paper 92-0001, Jan. 1992.

[7]Buckmaster, J., "The Structure and Stability of Laminar Flames," *Annual Review of Fluid Mechanics*, Vol. 25, 1993, pp. 21–54.

[8]Liñan, A., and Williams, F. A., *Fundamental Aspects of Combustion*, Oxford Univ. Press, Oxford, England, UK, 1993.

[9]Bertin, J. J., Periaux, J., and Ballman, J. (eds.), *Advances in Hypersonics, Defining the Hypersonic Environment*, Vol. 1, Birkhäuser, Boston, MA, 1992.

[10]Clarke, J. F., and McChesney, M., *The Dynamics of Real Gases*, Butterworths, London, 1964, p. 325.

[11]Landau, L., and Teller, E., "Zur Theorie der Schalldispersion," *Physik Zeitschrift der Sowjetunion*, Vol. 10, 1936, p. 34.

[12]Millikan, R. C., and White, D. R., "Systematics of Vibrational Relaxation," *Journal of Chemical Physics*, Vol. 39, 1963, pp. 3209–3213.

[13]Schwartz, R. N., Slawsky, Z. I., and Herzfeld, K. F., "Calculation of Vibrational Relaxation Times in Gases," *Journal of Chemical Physics*, Vol. 20, 1952, pp. 1591–1599.

[14]Treanor, C. E., Rich, J. W., and Rehm, R. G., "Vibrational Relaxation of Anharmonic Oscillations with Exchange-Dominated Collisions," *Journal of Chemical Physics*, Vol. 48, 1968, pp. 1798–1807.

[15]Rich, J. W., and Treanor, C. E., "Vibrational Relaxation in Gas-Dynamic Flows," *Annual Review of Fluid Mechanics*, Vol. 2, 1970, pp. 355–396.

[16]Park, C., "Estimation of Excitation Energy of Diatomic Molecules in Expanding Nonequilibrium Flows," AIAA Paper 92-0805, Jan. 1992.

[17]Ruffin, S. M., and Park, C., "Vibrational Relaxation of Anharmonic Oscillators in Expanding Flows," AIAA Paper 92-0806, Jan. 1992.

[18]de Gavelle de Roany, A. C., Flament, C., Rich, J. W., Subramanian, V. V., and Warren, W. R., Jr., "Strong Vibrational Nonequilibrium in Supersonic Nozzle Flows," *AIAA Journal*, Vol. 31, 1993, pp. 119–128.

[19]Sharma, S. P., Huo, W., and Park, C., "The Rate Parameters for Coupled Vibration-Dissociation in a Generalized SSH Approximation," AIAA Paper 88-2714, June 1988.

[20]Hammerling, P., Teare, J. D., and Kivel, B., "Theory of Radiation from Luminous Shock Waves in Nitrogen," *Physics of Fluids*, Vol. 2, 1959, pp. 422–426.

[21]Treanor, C. E., and Marrone, P. V., "Effect of Dissociation on the Rate of Vibrational Relaxation," *Physics of Fluids*, Vol. 5, 1962, pp. 1022–1026.

[22]Marrone, P. V., and Treanor, C. E., "Chemical Relaxation from Excited Vibrational Levels," *Physics of Fluids*, Vol. 6, 1963, pp. 1215–1221.

[23]Gonzales, D. A., and Varghese, P. L., "Vibrational Relaxation and Dissociation in Nitrogen," AIAA Paper 91-1370, June 1991.

[24]Schwartz, R. N., and Herzfeld, K. F., "Vibrational Relaxation Times in Gases (Three-Dimensional Treatment)," *Journal of Chemical Physics*, Vol. 22, 1954, pp. 767–773.

[25]Tanczos, F. I., "Calculation of Vibrational Relaxation Times of the Chloromethanes," *Journal of Chemical Physics*, Vol. 25, 1956, pp. 439–447.

[26]Landrum, D. B., and Candler, G., "Vibration-Dissociation Coupling in Nonequilibrium Flows," AIAA Paper 91-0466, Jan. 1991.

[27]Olynick, D. J., Moss, J. N., and Hassan, H. A., "Monte Carlo Simulation of Vibrational Relaxation in Nitrogen," AIAA Paper 90-1767, June 1990.

[28]Keck, J., and Carrier, G., "Diffusion Theory of Nonequilibrium Dissociation and Recombination," *Journal of Chemical Physics*, Vol. 43, 1965, pp. 2284–2298.

[29]Lee, J. H., "Electron-Impact Vibrational Relaxation in High-Temperature Nitrogen," AIAA Paper 92-0807, Jan. 1992.

[30]Lee, J. H., "Basic Governing Equations for the Flight Regimes of Aeroassisted Orbital Transfer Vehicles," *Thermal Design of Aeroassisted Orbital Transfer Vehicles*, edited by H. F. Nelson, Vol. 96, Progress in Astronautics and Aeronautics, AIAA, New York, 1985, pp. 3–53.

[31]Rapp, D., and Kassal, T., "Theory of Vibrational Energy Transfer Between Simple Molecules in Nonreactive Collisions," *Chemical Review*, Vol. 69, 1969, pp. 61–102.

[32]Gonzales, D. A., and Varghese, P. L., "Rate Calculations for the Simultaneous Vibrational Relaxation and Dissociation of Nitrogen," AIAA Paper 92-0808, Jan. 1992.

[33]Kunc, J. A., "Central-Force Potential for Interaction of Rotationally and Vibrationally Excited Molecules," *Journal of Physics B: Atomic, Molecular and Optical Physics*, Vol. 23, 1990, pp. 1–13.

[34]Kunc, J. A., "Vibration-Translation Exchange in Diatom-Diatom Collision," *Journal of Physics B: Atomic, Molecular and Optical Physics*, Vol. 24, 1991, pp. 3741–3761.

[35]Rich, J. W., and Macheret, S. O., "Aerothermodynamics of Vibrationally Nonequilibrium Gases," *Proceedings of the Third World Conference on Experimental Heat Transfer, Fluid Mechanics, and Thermodynamics* (Honolulu, HI), Nov. 1993.

[36]Gordiets, B. F., and Mamedov, S. S., "Isotope Separation in Chemical Reactions of Vibrationally Excited Molecules," *Soviet Journal of Quantum Electronics*, Vol. 5, 1976, pp. 1082–1084; see also Gordiets, B. F., and Mamedov, S. S., "Analytic Model for the Electric CO Laser," *Soviet Physics Technical Physics*, Vol. 22, 1977, pp. 498–502.

[37]Lam, S. H., "An Analytical Theory of Vibrational Relaxation for Anharmonic Molecules Under Strong Pumped Conditions," *Journal of Chemical Physics*, Vol. 67, 1977, pp. 2577–2584.

[38]Macheret, S. O., and Rich, J. W., "Nonequilibrium Dissociation Rates Behind Strong Shock Waves: Classical Model," *Journal of Chemical Physics* (to be published); see also AIAA Paper 93-2860, July 1993.

[39]Greendyke, R. B., and Hartung, L. C., "A Convective and Radiative Heat Transfer Analyses for the FIRE II Forebody," AIAA Paper 93-3194, July 1993.

[40]Cambier, J.-L., and Moreau, S., "Simulations of a Molecular Plasma in Collisional-Radiative Nonequilibrium," AIAA Paper 93-3196, July 1993.

[41]Gally, T. A., and Carlson, L. A., "Survey of Nonequilibrium Re-Entry Heating for Entry Flight Conditions," AIAA Paper 93-3230, July 1993.

[42]Tirsky, A. G., Shchelin, V. S., and Shcherbak, V. G., "The Influence of Uncertainty in Chemical Reaction on Convective Heat Transfer," *Izvestiya Akademii Nauk SSSR, Mekhanika Zhidkosti i Gaza*, Vol. 6, 1990, pp. 146–151.

[43]Yos, J. M., "Transport Properties of Nitrogen, Hydrogen, Oxygen, and Air to 30,000 K," AVCO Corp., TM RADTM-63-7, Wilmington, MA, 1963.

[44]Wilke, C. R., "Viscosity Equation for Gas Mixtures," *Journal of Chemical Physics*, Vol. 15, 1950, pp. 517–519.

[45]Kang, S. H., and Kunc, J. A., "Viscosity of High-Temperature Iodine," *Physical Review A*, Vol. 44, 1991, pp. 3596–3604.

[46]Kunc, J. A., "Analytical Dependence of the Viscosity Cross Sections and Viscosity Coefficients on Parameters of Intermolecular Potentials," *Journal of Chemical Physics*, Vol. 99, 1993, pp. 4705–4717.

[47]Gupta, R. N., "Navier–Stokes and Viscous Shock-Layer Solutions for Radiating Hypersonic Flows," AIAA Paper 87-1576, June 1987.

[48]Cauchon, D. L., "Radiative Heating Results from the Fire-II Flight Experiment at a Reentry Velocity of 11.4 km/sec," NASA TM X-1402, 1966.

[49]Sutton, K., "Air Radiation Revisited," *Thermal Design of Aeroassisted Orbital Transfer Vehicles*, edited by H. F. Nelson, Vol. 96, Progress in Astronautics and Aeronautics, AIAA, New York, 1985, pp. 419–441.

[50]Gnoffo, P. A., "Code Calibration Program in Support of the Aeroassisted Flight Experiment," *Journal of Spacecraft and Rockets*, Vol. 27, 1990, pp. 131–142.

[51]Hamilton, H. H., Gupta, R. N., and Jones, J. J., "Flight Stagnation-Point Heating Calculations of AFE Vehicle," *Journal of Spacecraft and Rockets*, Vol. 28, 1991, pp. 125–128.

[52]Gupta, R. N., Lee, K. P., Moss, J. N., and Sutton, K., "Viscous-Shock-Layer Solutions with Coupled Radiation and Ablation Injection for Earth Entry," AIAA Paper 90-1697, June 1990.

[53]Moss, J. N., "Radiative Shock Layer Solutions with Couple Ablation Injection," *AIAA Journal*, Vol. 14, 1976, pp. 1311–1317.

[54]Candler, G. V., "Computation of Thermo-Chemical Nonequilibrium Martian Atmospheric Entry Flows," AIAA Paper 90-1695, June 1990.

[55]Park, C., Howe, J. T., Jaffe, R. L., and Candler, G. V., "Chemical-Kinetic Problems of Future NASA Missions," AIAA Paper 91-0464, Jan. 1991.

[56]Gupta, R. N., Lee, K. P., Moss, J. N., and Sutton, K., "A Viscous-Shock-Layer Analysis of the Martian Aerothermal Environment," AIAA Paper 91-1345, June 1991.

[57]Jones, W. L., and Cross, A. E., "Electrostatic Probe Measurements of Plasma Parameters for Two Reentry Flight Experiments at 25,000 ft/sec," NASA TND-6617, 1972.

[58]Kang, S. W., Jones, W. L., and Dunn, M. G., "Theoretical and Measured Electron-Density Distributions at High Altitudes," *AIAA Journal*, Vol. 11, 1973, pp. 141–149.

[59]Gnoffo, P. A., Gupta, R. N., and Shinn, A. E., "Conservation Equations and Physical Models for Hypersonic Air Flows in Thermal and Chemical Nonequilibrium," NASA TP 2867, 1989.

[60]Howe, J. T., "Hypervelocity Atmospheric Flight: Real Gas Flow Field," NASA Reference Rept. 1249, Nov. 1990.

[61]Qu, Z. H., Shen, J. W., and Ruan, L. M., "The Effects of Different Diffusion Models on Electron Distribution in a Plasma Sheath About Reentry Bodies," *Journal of National University Defense Technology*, Vol. 15, 1993, pp. 31–37 (in Chinese).

[62]Candler, G. V., and MacCormack, R. N., "The Computation of Hypersonic Ionized Flows in Chemical and Thermal Nonequilibrium," AIAA Paper 88-0511, Jan. 1988.

[63]Greendyke, R. B., Gnoffo, P. A., and Lawrence, R. W., "Electron Number Density Profile for the Aeroassist Flight Experiment," AIAA Paper 92-0804, Jan. 1992.

[64]Dunn, M. G., and Kang, S. W., "Theoretical and Experimental Studies of Reentry Plasma," NASA CR-2232, 1973.

[65]Park, C., "Assessment of Two-Temperature Kinetic Model for Ionized Air," AIAA Paper 87-1574, June 1987.

[66]Hansen, C. F., "Collision-Induced Gas Phase Dissociation Rates," Final Rept., NASA Grant NAG 1-1046, 1990.

[67]Hartung, L. C., Mitcheltree, R. A., and Gnoffo, P. A., "Stagnation Point Nonequilibrium Radiative Heating and the Influence of Energy Exchange Models," AIAA Paper 91-0571, Jan. 1991.

[68]Mitcheltree, R. A., "A Parametric Study of Dissociation and Ionization Models at 12 km/sec," AIAA Paper 91-1368, June 1991.

[69]Hartung, L. C., "Development of a Nonequilibrium Radiative Heating Prediction Method for Coupled Flowfield Solutions," AIAA Paper 91-1406, June 1991.

[70]Allen, R. A., Rose, P. H., and Camm, J. C., "Nonequilibrium and Equilibrium Radiation at Super-Satellite Reentry Velocities," AVCO Everett Research Lab. Rept. RR 156, 1962.

[71]Sherman, F. S., "The Transition from Continuum to Molecular Flow," *Annual Review of Fluid Mechanics*, Vol. 1, 1969, pp. 317–340.

[72]Kogan, M. N., "Molecular Gas Dynamics," *Annual Review of Fluid Mechanics*, Vol. 5, 1973, pp. 383–404.

[73]Bird, G. A., "Monte Carlo Simulation of Gas Flows," *Annual Review of Fluid Mechanics*, Vol. 10, 1978, pp. 11–31.

[74]Muntz, E. P., "Rarefied Gas Dynamics," *Annual Review of Fluid Mechanics*, Vol. 21, 1989, pp. 387–417.

[75]Lin, T. C., McGregor, R. D., Wong, J. L., and Grabowsky, W. R., "Numerical Simulation of 3D Rarefied Hypersonic Flows," AIAA Paper 89-1715, June 1989.

[76]Bird, G. A., *Molecular Gas Dynamics*, Clarendon Press, Oxford, England, UK, 1976.

[77]Bird, G. A., "Simulation of Multi-Dimensional and Chemically Reacting Flow," *Rarefied Gas Dynamics*, edited by R. Campargue, Vol. 1, 1979, pp. 365–388.

[78]Bird, G. A., "Low Density Aerothermodynamics," AIAA Paper 85-0994, June 1985.

[79]Bird, G. A., "Perception of Numerical Methods in Rarefied Gasdynamics," *Rarefied Gas Dynamics: Theoretical and Computational Techniques*, Vol. 118, Progress in Astronautics and Aeronautics, AIAA, Washington, DC, 1989, pp. 221–226.

[80]Furlani, T. R., and Lordi, J., "A Comparison of Parallel Algorithms for the Direct Simulation Monte Carlo Method. II—Application to Exhaust Plume Flowfields," AIAA Paper 89-1667, June 1989.

[81]Baganoff, D., and McDonald, J. D., "A Collision-Selection Rule for a Particle Simulation Method Suited to Vector Computers," *Physics of Fluids A*, Vol. 2, 1990, pp. 1248–1259.

[82]Boyd, I. D., "Analysis of Vibrational-Translational Energy Transfer Using the Direct Simulation Monte Carlo Method," *Physics of Fluids A*, Vol. 3, 1991, pp. 1785–1791.

[83]Wilmoth, R. G., "Application of Parallel DSMC Method to Hypersonic Rarefied Flows," AIAA Paper 91-0772, Jan. 1991, and "Direct Simulation Monte Carlo Analysis on Parallel Processors," AIAA Paper 89-1666, June 1989.

[84]McDonald, J. D., "Particle Simulation in a Multiprocessor Environment," AIAA Paper 91-1366, June 1991.

[85]Borgnakke, C., and Larson, P. S., "Statistical Collision Model for Monte Carlo Simulation of Polyatomic Gas Mixture," *Journal of Computational Physics*, Vol. 18, 1975, pp. 405–420.

[86]Olynick, D. J., Moss, J. N., and Hassan, H. A., "Monte Carlo Simulation of Nonequilibrium Shock Fronts," AIAA Paper 91-1341, June 1991.

[87]Boyd, I. D., "Rotational-Translational Energy Transfer in Rarefied Nonequilibrium Flows," *Physics of Fluids A*, Vol. 2, 1990, pp. 447–452.

[88]Parker, J. G., "Rotational and Vibrational Relaxation in Diatomic Gases," *Physics of Fluids*, Vol. 2, 1959, pp. 449–462.

[89]Chung, C. H., DeWitt, K. J., and Jeng, D. R., "A New Approach in Direct-Simulation of Gas Mixtures," AIAA Paper 91-1343, June 1991.

[90]Gibson, W. E., and Marrone, P. V., "Correspondence Between Normal Shock and Blunt Body Flow," *Physics of Fluids*, Vol. 5, pp. 1649–1656.

[91]Hall, J. G., Eschenroeder, A. A., and Marrone, P. V., "Blunt Nosed Inviscid Air Flows with Coupled Nonequilibrium Processes," *Journal of Aerospace Sciences*, Vol. 29, 1962, pp. 1038–1051.

[92]Bird, G. A., "Nonequilibrium Radiation During Re-Entry at 10 km/s," AIAA Paper 87-1543, June 1987.

[93]Moss, J. N., Bird, G. A., and Dogra, V. K., "Nonequilibrium Thermal Radiation for an Aeroassist Flight Experiment Vehicle," AIAA Paper 88-0081, Jan. 1988.

[94]Carlson, A. B., and Hassan, H. A., "Radiation Modelling with Direct Simulation Monte Carlo," AIAA Paper 91-1409, June 1991.

[95]Boyd, I. D., Penko, P. F., and Meissner, D. L., "Numerical and Experimental Investigations of Rarefied Nozzle and Plume Flows of Nitrogen," AIAA Paper 91-1363, June 1991.

[96]Pham-Van-Diep, G. C., "Chemically Reacting Hypersonic Flows of Iodine Vapor for the Study of Nonequilibrium Phenomena in Diatomic Gases," Ph.D. Dissertation, Dept. of Aerospace Engineering, Univ. of Southern California, Los Angeles, CA, 1993.

[97]Boyd, I. D., Pham-Van-Diep, G. C., and Muntz, E. P., "Monte Carlo Computation of Nonequilibrium Flow in Hypersonic Iodine Wind Tunnel," AIAA Paper 93-2871, July 1993.

[98]Pham-Van-Diep, G. C., Muntz, E. P., and Boyd, I. D., "Measurement of Rotational and Vibrational Population Distributions in a Hypersonic Flow of Chemically Reacting Iodine Vapor," AIAA Paper 93-1996, June 1993.

[99]Emanuel, G., *Gasdynamics: Theory and Applications*, AIAA Education Series, New York, 1986, pp. 387–396.

[100]Carlson, A. B., and Wilmoth, R. G. "Shock Interference Prediction Using Direct Simulation Monte Carlo," AIAA Paper 92-0492, Jan. 1992.

[101]Weiting, A., and Holden, M. S., "Experimental Study of Shock-Wave Interference Heating on a Cylinder at Mach 6 and 8," *AIAA Journal*, Vol. 27, 1989, pp. 1557–1565.

[102]Dogra, V. K., Moss, J. N., Wilmoth, R. G., and Price, J. M., "Hypersonic Rarefied Flow Past Spheres Including Wake Structure," AIAA Paper 92-0495, Jan. 1992.

[103]Legge, H., and Koppenwallner, G., "Sphere Drag Measurement in Free Jet in a Hypersonic Low-Density Wind Tunnel," DF-UVFL-UREV Rept. 70A 37a, 1970.

[104]Campbell, D. H., "DSMC Analysis of Plume-Freestream Interactions and Comparison of Plume Flowfield Predictions with Experimental Measurements," AIAA Paper 91-1362, June 1991.

[105]Celenligil, M. C., and Moss, J. N., "Hypersonic Rarefied Flow about a Delta Wing-Direct Simulation and Comparison with Experiment," AIAA Paper 91-1315, June 1991.

[106]Rault, D. F. G., "Aerodynamic Characteristics of a Hypersonic Viscous Optimized Waverider at High Altitudes," AIAA Paper 92-0306, Jan. 1992.

[107]Bird, G. A., "Application of the Direct Simulation Monte Carlo Method to the Full Shuttle Geometry," AIAA Paper 90-1692, June 1990.

[108]Bird, G. A., *The F3 Program System User's Manual*, G.A.B. Consulting, Ply. Ltd., 1990.

[109]Celenligil, M. C., Moss, J. N., and Blanchard, R. C., "Three-Dimensional Rarefied Flow Simulations for the Aeroassist Flight Experiment," *AIAA Journal*, Vol. 29, 1991, pp. 52–57.

[110]Erwin, D. A., Pham-Van-Diep, G. C., and Muntz, E. P., "Nonequilibrium Gas Flows. I: A Detailed Validation of Monte Carlo Direct Simulation for Monatomic Gases," *Physics of Fluids A*, Vol. 3, 1991, pp. 697–705.

[111]Pham-Van-Diep, G. C., Erwin, D. A., and Muntz, E. P., "Nonequilibrium Molecular Motion in a Hypersonic Shock Wave," *Science*, Vol. 245, Aug. 1989, pp. 624–626.

[112]Pham-Van-Diep, G. C., Erwin, D. A., and Muntz, E. P., "Testing Continuum Descriptions of Low-Mach-Number Shock Structures," *Journal of Fluid Mechanics*, Vol. 232, 1991, pp. 403–413.

[113]Maitland, G. C., Rigby, M., Smith, E. B., and Wakeham, W. A., *Intermolecular Forces*, Clarendon Press, Oxford, England, UK, 1981.

[114]Mott-Smith, H. M., "The Solution of the Boltzmann Equation for a Shock Wave," *Physical Review*, Vol. 82, 1951, pp. 885–887.

[115]Muntz, E. P., Erwin, D. A., and Pham-Van-Diep, G. C., "A Review of the Kinetic Detail Required for Accurate Predictions of Normal Shock Waves," *Proceedings of the 17th International Rarefied Gas Dynamics Symposium*, (Aachen, Germany), edited by A. E. Beylich, 1990, pp. 198–206.

[116]Wadsworth, D. C., Muntz, E. P., Blackwelder, R. F., and Shiflett, G. R., "Transient Energy Release Pressure Driven Microactuators for Control of Wall-Bound Turbulent Flows," AIAA Paper 93-3271, July 1993.

[117]Wadsworth, D. C., "Microscale Gas Dynamics," Ph.D. Dissertation, Dept. of Aerospace Engineering, Univ. of Southern California, Los Angeles, CA, 1993.

[118]Cheng, H. K., "The Blunt-Body Problem in Hypersonic Flow at Low Reynolds Number," Cornell Aeronautical Lab., Rept. AF-1285-A-10, 1963.

[119]Cheng, H. K., "Viscous Hypersonic Blunt-Body Problem and the Newtonian Theory," *Fundamental Phenomena in Hypersonic Flow*, edited by G. J. Hall, Cornell Univ. Press, Ithaca, NY, 1966, pp. 91–132.

[120]Wilson, M. R., and Wittliff, C. E., "Low Density Stagnation Point Heat Transfer Measurements in the Hypersonic Shock Tunnel," *ARS Journal*, Vol. 32, 1962, pp. 275–276.

[121]Vidal, R. J., Golian, T. C., and Bartz, J. A., "Shock Tunnel Heat-Transfer and Pressure Data Show Viscous Effects on a Low-Density Hypersonic Flow Past a Sharp Flat Plate at Various Attack Angles," AIAA Paper 63-435, Jan. 1963.

[122]Moss, J. N., and Bird, G. A., "Direct Simulation of Translational Flow for Hypersonic Reentry Conditions," *Thermal Design of Aeroassisted Orbital Transfer Vehicles*, edited by H. F. Nelson, Vol. 96, Progress in Astronautics and Aeronautics, AIAA, New York, 1985, pp. 113–139.

[123]Gupta, R. N., and Simmonds, A. L., "Hypersonic Low-Density Solutions of the Navier–Stokes Equations with Chemical Nonequilibrium and Multicomponent Surface Slip," AIAA Paper 86-1349, June 1986.

[124]Moss, J. N., Cuda, V., and Simmonds, A. L., "Nonequilibrium Effects for Hypersonic Transitional Flows," AIAA Paper 87-0404, Jan. 1987.

[125]Borodin, A. I., and Peigin, S. V., "Three-Dimensional Thin Shock Layer in the Absence of a Plane of Symmetry in the Flow," *Izvestiya Akademii Nauk SSSR, Mekhanika Zhidkosti i Gaza*, 1989, pp. 150–158 (English translation by Plenum Pub. Corp.).

[126]Davis, R. T., "Numerical Solution of the Hypersonic Viscous Shock-Layer Equations," *AIAA Journal*, Vol. 8, 1970, pp. 843–851.

[127]Cheng, H. K., "Hypersonic Shock-Layer Theory of the Stagnation Region at Low Reynolds Number," *Proceedings of the Heat Transfer and Fluid Mechanics Institute*, edited by R. C. Bender et al., Stanford Univ. Press, Palo Alto, CA, 1961, pp. 161–175.

[128]Lee, K. P., Gupta, R. N., Zoby, E. V., and Moss, J. N., "Hypersonic Shock Layer Solutions Over Long Slender Bodies—Part II. Low Reynolds Number Flows," *Journal of Spacecraft and Rockets*, Vol. 27, 1990, pp. 185–193.

[129]Gupta, R. N., Jones, J. J., and Rochelle, W. C., "Stagnation-Point Heat-Transfer Rate Predictions at Aeroassisted Flight Conditions," NASA TP 3208, 1992.

[130]Burnett, D., "The Distribution of Molecular Velocities and the Mean Motion in a Non-uniform Gas," *Proceedings of the London Mathematical Society*, Vol. 40, 1936, pp. 382–435.

[131]Grad, H., "On the Kinetic Theory of Rarefied Gases," *Communications on Pure and Applied Mathematics*, Vol. 2, 1949, pp. 331–407.

[132]Shaaf, S. A., and Chambré, P. L., "Flow of Rarefied Gases," *Fundamentals of Gas Dynamics*, edited by H. W. Emmons, Sec. H., Princeton Univ. Press, Princeton, NJ, 1958, pp. 687–739.

[133]Fiscko, K. A., and Chapman, D. R., "Hypersonic Shock Structure with Burnett Terms in the Viscous Stress and Heat Flux," AIAA Paper 88-2733, June 1988.

[134]Fiscko, K. A., and Chapman, D. R., "Comparison of Burnett, Super-Burnett and Monte Carlo Solutions for Hypersonic Shock Structure," *Rarefied Gas Dynamics: Theoretical and Computational Techniques*, Vol. 118, Progress in Astronautics and Aeronautics, AIAA, Washington, DC, 1989, pp. 374–395.

[135]Chapman, S., and Cowling, T. G., *The Mathematical Theory of Nonuniform Gases*, Cambridge Univ. Press, New York, 1953.

[136]Vincenti, W. G., and Kruger, C. H., Jr., *Introduction to Physical Gas Dynamics*, Wiley, New York, 1965.

[137]Ferziger, J. H., and Kaper, H. G., *Mathematical Theory of Transport Processes in Gases*, North-Holland, Amsterdam, 1972.

[138]Simon, C. E., "Theory of Shock Structure in a Maxwell Gas Based on Chapman-Enskog Development Through Super-Burnett Order," Ph.D. Dissertation, Univ. of Colorado, Boulder, CO, 1976.

[139]Woods, L. C., "Frame-Indifferent Kinetic Theory," *Journal of Fluid Mechanics*, Vol. 136, 1983, pp. 423–433.

[140]Yang, H. T., "Reduction of Grad's Thirteen-Moment Equations and Boundary Conditions to Burnett's Equations and Corresponding Boundary Conditions," Univ. of Southern California, Dept. of Aerospace Engineering, Rept. USCAE 152, Los Angeles, CA, 1992.

[141]Grad, H., "The Profiles of a Steady Plane Shock Wave," *Communications of Pure and Applied Mathematics*, Vol. 5, 1952, pp. 257–300.

[142]Garen, W., Synofzik, R., and Wortberg, G., "Experimental Investigation of the Structure of Weak Shock Waves in Noble Gases," Vol. 51, Progress in Astronautics and Aeronautics, AIAA, New York, 1977, pp. 519–528.

[143]Bobylev, A. V., "The Chapman-Enskog and Grad Methods for Solving the Boltzmann Equation," *Soviet Physics—Doklady*, Vol. 27, 1982, pp. 29–31.

[144]Foch, J. D., Jr., "On Higher Order Hydrodynamic Theories of Shock Structure," *The Boltzmann Equations*, edited by E. G. D. Cohen and W. Thirring, Springer–Verlag, Vienna, 1973, pp. 123–140.

[145]Zhong, X., MacCormack, R. W., and Chapman, D. R., "Stabilization of the Burnett Equations and Applicaton to Hypersonic Flow," *AIAA Journal*, Vol. 31, 1993, pp. 1036–1043.

[146]Zhong, X., MacCormack, R. W., and Chapman, D. R., "Evaluation of Slip Boundary Conditions for the Burnett Equations with Application to Hypersonic Leading Edge Flow," *Proceedings of the 4th International Symposium on Computational Fluid Dynamics* (Davis, CA), 1991.

[147]Wang-Chang, C. S., and Uhlenbeck, G. E., "Transport Phenomena in Polyatomic Gases," Univ. of Michigan, Engineering Research Inst., Rept. CM-681, Project M604-6, Ann Arbor, MI, 1951.

[148]Lee, C. J., "On the Unique Determination of Solutions to the Burnett Equations," *AIAA Journal*, Vol. 32, 1994, pp. 985–990.

[149]Zhong, X., "On Numerical Solutions of the Burnett Equations for Hypersonic Flow Past 2-D Circular Blunt Leading Edges in Continuum Transition Regime," AIAA Paper 93-3092, July 1993.

[150]Schamberg, R., "The Fundamental Differential Equations and the Boundary Conditions for High Speed Slip Flow," Ph.D. Dissertation, California Inst. of Technology, Pasadena, CA, 1947.

[151]Cheng, H. K., Lee, C. J., Wong, E. Y., and Yang, H. T., "Hypersonic Slip Flows and Issues on Extending Continuum Model Beyond the Navier–Stokes Level," AIAA Paper 89-1663, June 1989.

[152]Cheng, H. K., Wong, E. Y., and Dogra, V. K., "A Shock-Layer Theory Based on Thirteen-Moment Equations and DSMC Calculations of Rarefied Hypersonic Flows," AIAA Paper 91-0783, Jan. 1991.

[153]Cheng, H. K., and Wong, E. Y., "Fluid Dynamic Modeling and Numerical Simulation of Low-Density Hypersonic Flows," Univ. of Southern California, Dept. of Aerospace Engineering, Rept. USCAE 147, Los Angeles, CA, 1988.

[154]Kuznetsov, M. M., and Kikol'skii, V. S., "Kinetic-Theory Analysis of Hypersonic Viscous Flows of a Polyatomic Gas in a Thin Three-Dimensional Shock Layer," *Central Aerohydrodynamic Institute Pub.*, Vol. 16, 1985, pp. 38–49 (in Russian).

[155]Wong, E. Y., "An Extension of the Continuum Model to Rarefied Hypersonic Flow with Grad's Thirteen-Moment Equations," Ph.D. Dissertation, Univ. of Southern California, Dept. of Aerospace Engineering, Los Angeles, CA, 1993.

[156]Cheng, H. K., Wong, E. Y., Hoover, L. N., and Dogra, V. K., "Flat Plate at Incidence as a Waverider in Rarefied Hypersonic Flow," *Proceedings of the First International Hypersonic Waverider Symposium*, Univ. of Maryland, College Park, MD, 1990.

[157]Cheng, H. K., "On a Hypersonic Shock Layer and Its Extension Beyond the Navier–Stokes Level," *Proceedings of the International Conference on Hypersonic Aerodynamics*, Univ. of Manchester, England, 1989, pp. 15–1 through 15–16.

[158]Dogra, V. K., and Moss, J. N., "Hypersonic Rarefied Flow About Plates at Incidence," AIAA Paper 89-1712, June 1989.

[159]Cheng, H. K., "The Thin Layer Approximation in Rarefied Hypersonic Gas Dynamics," *Proceedings of the Fourth International Symposium on Computational Fluid Dynamics* (Davis, CA), 1991, pp. 178–185.

[160]Warr, J., "Orbital Aerodynamic Computer Program to Calculated Force and Moment Coefficients on Complex Vehicle Configurations," Lockheed, LMSC/HREC D 1624 98 TM 54-20-275, Houston, TX, 1970.

[161]Wilhite, A. W., Airington, J. P., and McCandless, R. S., "Performance Aerodynamics of AOTV," *Thermal Design of Aeroassisted Orbital Transfer Vehicles*, edited by H. F. Nelson, Vol. 96, Progress in Astronautics and Aeronautics, AIAA, New York, 1985, pp. 165–197.

[162]Potter, L. J., "Procedure for Estimating Aerodynamics of Three-Dimensional Bodies in Transitional Flow," *Rarefied Gas Dynamics: Theoretical and Computational Techniques*, Vol. 118, Progress in Astronautics and Aeronautics, AIAA, Washington, DC, 1988, pp. 482–492.

[163]Holden, M. S., "A Database Compiled from Heat-Transfer Measurements Made in Hypersonic Flows for CFD Validation," AIAA Paper 92-4023, July 1992.

[164]Hornung, H., Sturtevant, B., Belanger, B., Sanderson, S., Mrouillette, M., and Jenkine, M., "Performance Data of the New Free-Piston Shock Tunnel T5 at GALCIT," *Proceedings of the 18th International Symposium on Shock Waves*, Springer–Verlag, New York, 1990, pp. 603–610.